CLINICALLY IMPORTANT

Nanomedicine: Nanotechnology, Biology, and Medicine
11 (2015) 795–810

Review Article

nanomedjournal.com

Radionanomedicine: Widened perspectives of molecular theragnosis

Dong Soo Lee, M.D., Ph.D.[a,b,*], Hyung-Jun Im, M.D.[b], Yun-Sang Lee, Ph.D.[a,b]

[a]*Department of Nuclear Medicine, College of Medicine, Seoul National University, Seoul, Republic of Korea*
[b]*Department of Molecular Medicine and Biopharmaceutical Sciences, Graduate School of Convergence Science and Technology, and College of Medicine or College of Pharmacy, Seoul National University, Seoul, Republic of Korea*

Received 21 August 2014; accepted 18 December 2014

Abstract

Despite of promising preclinical results in the fields of *in vivo* theragnostics of nanomedicine, a majority of attempt for clinical translation has been blocked by unsolved concerns about possible hazards to human body. Theragnosis of nanomedicine relies on the property of huge surface area to volume ratio of nanomaterials, which can offer potential for multi-functionality. Radionanomedicine has a hybrid characteristic of tracer technology and multi-functionality. Thus, key advantage of radionanomedicine is a possibility of using low amount of nanomaterials for theragnosis. This review article focuses on the concept and advantages of radionanomedicine in theragnosis, formulation of radionanomaterials (particularly encapsulation method), in vivo biodistribution and excretion of radionanomaterials, and immune responses to radionanomaterials.

From the Clinical Editor: The expansion of nanomedicine has recently seen the development of a new branch - radionanomedicine. The core concept of radionanomedicine relies on the labeling of radionuclides onto nanomaterials for use both in diagnosis and therapy. In this article, the authors gave a comprehensive review on the current status of radionanomedicine. This should provide interesting reading for practicing clinicians.

Key words: Nanomedicine; Radiolabeling; Theragnosis; Encapsulation; Biodistribution

Nanomedicine consists of the following four disciplines: *in vitro* nanosensing and diagnostics, nanomolecular imaging, nano-targeted delivery, and tissue nano-engineering. Among them, *in vivo* theragnostics with or without imaging are related to nanomolecular imaging and nano-targeted delivery. It is predicted that *in vitro* diagnostics using nanotechnology will be used in clinical applications in the near future. Incremental values or comparative effectiveness of the new *in vitro* nanodiagnostic tools will determine their use. In contrast, *in vivo* theragnostics using nanotechnology meets objections or concerns about the possible hazards to humans and the environment.[1-4] There is a need to develop methods and ways to overcome the concerns about the toxic effects of the *in vivo* use of nanomaterials.

The concept of radionanomedicine was recently presented as an extension of "targeted radionuclide therapy" in international symposia of the ICRT2012 (International Conference for Radiopharmaceutical Therapy), ISRS2013 (International Symposium of Radiopharmaceutical Sciences), 2014 international symposium of the NCC (National Cancer Center), and WCNMB2014 (World Congress of Nuclear Medicine and Biology). The core concept of radionanomedicine relies on both the labeling of radionuclides onto the nanomaterials and the use of trace amounts of radiolabeled nanomaterials for *in vivo* theragnostics. First, the labeling of nanomaterials with radionuclides can be achieved in two ways: extrinsically, using chelators bound to the surface of nanomaterials,[5] and intrinsically, inside the nanoparticle[6,7] (Figure 1). Representative examples of intrinsically and extrinsically labeled nanoparticles are summarized in Table 1. Studies regarding intrinsically radiolabeled nanoparticles are well summarized in a recent review article by Goel et al.[52] In 2010, Zhou et al developed intrinsically ^{64}Cu-labeled copper sulfide (CuS) and the nanoparticle showed passive targeting in mouse tumor model.[8] In 2011, intrinsically radioactive upconverting nanoparticle, [^{18}F]-$NaYF_4$:Gd,Yb,Er, was developed.[22] In 2014, Zhao et al developed a gold nanoparticle intrinsically labeled with ^{64}Cu and showed passive targeting of the nanoparticle to breast cancer mouse model.[10] Extrinsically labeled nanoparticles using chelators according to labeling methods and materials are well summarized in recent review articles by Xing et al[53] and Enrique et al[54] Chelators used

Conflict of interest: The authors declare that they have no conflict of interest.

*Corresponding author at: Department of Nuclear Medicine, Seoul National University Hospital 101 Daehangno Jongnogu, Seoul 110-744, Korea.
E-mail address: dsl@plaza.snu.ac.kr (D.S. Lee).

http://dx.doi.org/10.1016/j.nano.2014.12.010
1549-9634/

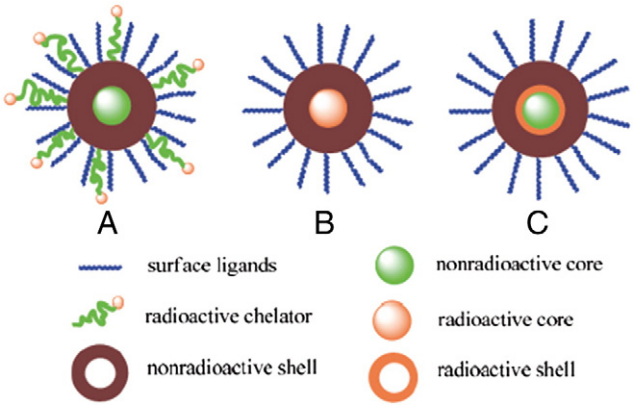

Figure 1. The core or the surface of the nanomaterials can be labeled with radioisotopes. The surface of the nanomaterials is linked to chelators, followed by labeling with radioisotopes. (Reprinted with permission from Ref.[6]).

reactor-produced ^{90}Y,[63] and generator-produced ^{188}Re.[64,65] The former three radioisotopes are used for diagnostic and the latter three for therapeutic purposes. In 2007, Cai et al labeled quantum dot (QD) with ^{64}Cu (^{64}Cu-DOTA-QD-RGD) with conjugation of DOTA and RGD peptides. ^{64}Cu-DOTA-QD-RGD showed better integrin positive tumor targeting than ^{64}Cu-DOTA-QD.[31] In 2011, Zhang et al developed polyethylene glycol-coated, core cross-linked polymeric micelles (CCPM) conjugated with ^{111}In-labeled annexin A5 for dual-modality single photon emission computed tomography/near-infrared fluorescence (SPECT/NIRF) tumor imaging.[43] Interestingly, therapeutic radioisotopes, ^{177}Lu and ^{188}Re can be used for diagnostic imaging as well. They are inherently theragnostic radioisotopes as they emit both beta and gamma rays. In 2004, Cao et al had labeled ^{188}Re on their surface of silica-coated magnetite nanoparticles immobilized with histidine with labeling yield of 91%.[46] Liang et al in 2007 reported ^{188}Re labeled super-

Table 1
Representative examples of radiolabeled nanoparticles.

Radiolabeling	Radioisotope (half-life)	Nanoparticles	Chelator	Therapy	Imaging method	References
Intrinsic	^{64}Cu (12.7 hr)	CuS	N	Y	PET/CT	8
		IO	N	N	PET/MR	9
		Gold	N	N	PET/CT	10
		Ferritin nanocage	N	N	PET/CT	11
		Porphysomes	N	N	PET/CT	12
	^{198}Au(2.69 d)	Gold	N	Y	SPECT/MR	13-17
		Gold nanocages	N	N	CL	18
	^{153}Sm (46.3 hr)	Ln doped NP	N	N	SPECT/ULI	19,20
	^{109}Cd (461.4 d)	QD	N	N	NIRF	6
	^{111}In (2.8 d)	IO	N	N	SPECT/CT	21
	^{18}F (109.8 min)	Ln doped NP	N	N	PET/ULI	22,23
	^{72}As (12.6 hr)	IO	N	N	PET/MR	24
	^{69}Ge (39.05 hr)	IO	N	N	PET/MR	25
Extrinsic	^{99m}Tc (6 hr)	Gold	Hynic	N	SPECT/CT	26-28
			DTPA	N	SPECT/CT	29
		IO	DTPA	N	SPECT/MR	30
	^{64}Cu (12.7 hr)	QD	DOTA	N	PET/NIRF	31,32
		IO	DOTA	N	PET/MR	33-36
		Carbon nanotube	DOTA	N	PET/NIRF	37
		Gold nanoshell	DOTA	Y	PET/CT	33
		Liposome	DOTA	N	PET/CT	38
	^{111}In (2.8 d)	Carbon nanotube	DTPA	N	SPECT/CT	39-41
			DOTA	N	SPECT/CT	42
		Micelle	DTPA	N	SPECT/CT	43
	^{124}I (4.18 d)	IO	Iodo-bead	N	PET/MR/CL	44
		Ln doped NP	Iodo-bead	N	PET/MR/ULI	45
	^{188}Re (16.9 hr)	IO	[M(CO)3(OH2)3]+	Y	SPECT/MR	46,47
		Liposome	BMEDA	Y	SPECT/CT	48
	^{177}Lu (6.73 d)	Gold	DOTA	Y	SPECT/CT	49
	^{68}Ga (67.7 min)	QD	DOTA	N	PET/CT	50
	^{67}Ga (78.3 hr)	Cobalt-ferrite	NOTA	N	SPECT/MR	51

QD = Quantum dot; IO = Iron oxide; Ln = lanthanide; CL = Cerenkov luminescence; ULI = Upconversion luminescence imaging; NIRF = Near-infrared Fluorescence; BMEDA = N,N-bis(2-mercaptoethyl)-N′,N′-diethylethylenediamine; Y = yes; N = no.

for this purpose include DTPA (diethylene triamine pentaacetic acid), DOTA (1,4,7,10-tetraazacyclododecane-1,4,7,10-tetraacetic acid), NOTA (1,4,7-triazacyclononane-1,4,7-triacetic acid), and others[55,56] (Figure 2). Commonly used radioisotopes range from generator-produced ^{68}Ga,[57] cyclotron-produced ^{64}Cu[58,59] or ^{89}Zr,[60] reactor-produced ^{177}Lu,[61,62] generator or paramagnetic iron oxide nanoparticles (SPIONs) with a greater than 90% labeling efficiency and a good in vitro stability. The NP demonstrated the dose dependent in vitro therapeutic ability in hepatocellular carcinoma cells.[47]

When a radionanomaterial has no therapeutic radiation-emitter within but nanomaterial itself has photothermal effect, this

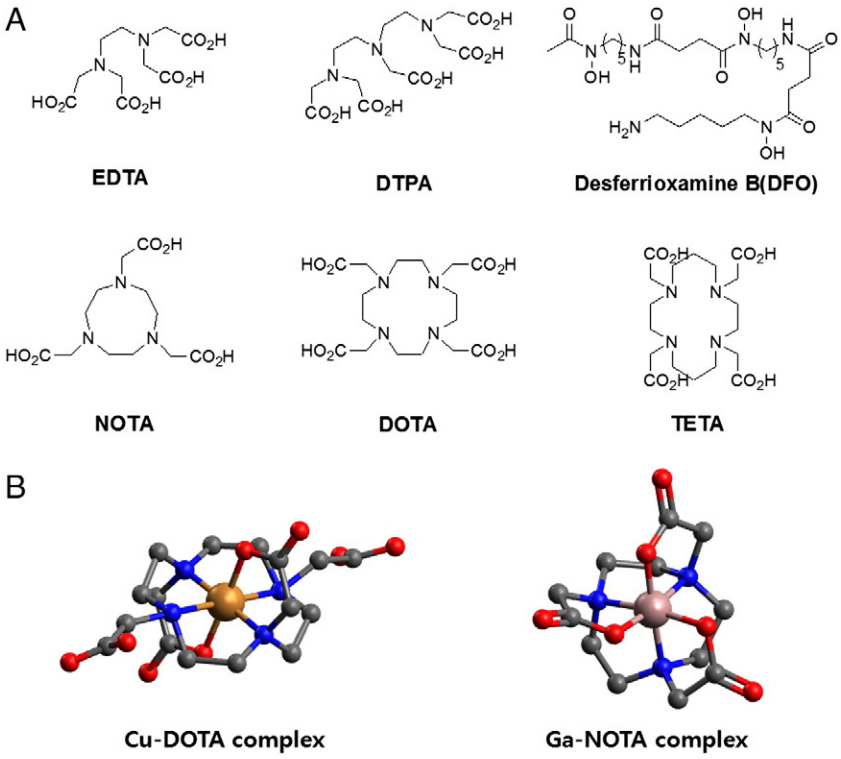

Figure 2. Structures of the chelators frequently used for PET radioisotopes such as ^{68}Ga, ^{64}Cu, and ^{89}Zr. **(A)** The structures of EDTA, DTPA, DOTA, NOTA, TETA and DFO. **(B)** ^{64}Cu is shown to be positioned with the chelator DOTA and ^{68}Ga with NOTA. (Reprinted with permission from Ref.[55]). DTPA: diethylene triamine pentaacetic acid, DOTA: 1,4,7,10-tetraazacyclododecane-1,4,7,10-tetraacetic acid, NOTA: 1,4,7-triazacyclononane-1,4,7-triacetic acid, DFO: deferroxamine or desferrioxamine B.

radionanomaterial also belongs to radionanomedicine. Radioisotope imaging using a radionanomaterial along with its photothermal ablation (PTA) effect is an example. Zhou et al developed a chelator-free [^{64}Cu]CuS nanoparticles (NPs) suitable both for PET imaging and as photothermal ablation agents.[8] Xie et al in 2011, developed ^{64}Cu labeled gold nanoshells, with integrin αvβ3 moiety to target tumor neoangiogenesis, whose gold nanoshell was for PTA. This was evaluated as a potential theragnostic approach for PET imaging and PTA.[33] In 2013, Luna-Guierrez et al developed ^{177}Lu labeled, gold nanoparticles conjugated to cyclo-[RGDfK(C)] peptides (^{177}Lu-AuNP-c[RGDfK(C)]) for both targeted radiotherapy and photothermal therapy. They showed in vitro therapeutic efficacy in breast cancer cell.[49]

Nanomaterials with proper type of intrinsic radioactivity can be used for both imaging and therapy. ^{198}Au/^{199}Au is one prime example of the strategy. The radioactive properties of ^{198}Au (beta ray = 0.96 MeV, gamma ray = 411 KeV) and ^{199}Au (beta ray = 0.46 MeV, gamma ray = 158 KeV) make them ideal candidates for use in theragnostic applications.[13] Khan et al reported therapeutic effect of ^{198}Au composite nanodevices in mouse melanoma tumor model by intratumoral injection of the nanomaterial.[14] Chanda et al reported that gum arabic glycoprotein (GA)-functionalized ^{198}Au showed therapeutic effect in mouse prostate cancer model after intratumoral injection of the nanoparticles. They also showed the biocompatibility of their approach by showing no or minimal leakage of the nanoparticles and no pathologic change in blood cells after the treatment.[15] In 2012, Shukla et al developed prostate tumor specific epigallocatechin-gallate (EGCg) functionalized ^{198}Au (^{198}Au NP-EGCg). In the study, ^{198}Au NP-EGCg was injected in prostate cancer mouse model. Approximately 72% NP retention was found in the tumor after 24 hours and 80% reduction of the tumor volume was found after 28 days.[16]

In addition, when these theragnostic radiolabeled nanomaterials are used in trace amounts, toxic effects of nanomaterials might not be worried about, though these nanomaterials are toxic by themselves in the pharmacologic amounts they are used. Compared with when the drugs were loaded within the nanomaterials,[66] if therapeutic radionuclides are bound to the nanomaterials, it should be possible to decrease the amount of nanomaterials to the minimum.

Radionanomedicine takes advantage of using nanomaterials whose surface can be used for labeling ligands and chelators and of the high sensitivity of radionuclides to be detected in the body. In this sense, radionanomedicine will follow the success of nuclear medicine. Nuclear medicine is a discipline of clinically successful applications of physiologic studies. The clinical physiology of the human body has been made visible by nuclear medicine diagnostic procedures and therapeutic success has been achieved by the target specificity of radionuclides and radiochemicals. Best examples of target specificity are the use of ^{131}I for thyroid cancer[67] or ^{223}Ra (Xofigo®, Bayer HealthCare Pharmaceuticals, Germany) for metastatic bone cancer.[68] For diagnostic purposes, nuclear medicine physicians successfully used small molecules and biomacromolecules in the

clinic. And the best examples of diagnostic small molecules are ^{99m}Tc-labeled phosphonates for bone scan imaging and ^{18}F fluorodeoxyglucose for positron emission tomography (PET) for tumors, myocardium and brain, and the best example of biomacromolecule is a monoclonal antibody such as ^{131}I-Tositumomab. The development of the methods enabling surface labeling with ligands and chelators is the problem to solve first; the development of the imaging methods to trace the whereabouts of the *in vivo*-administered radiolabeled nanomaterials is the next problem to solve. These two improvements, if successfully achieved, will lead to the successful translation of the use of radiolabeled nanomaterials to clinical applications in the near future. In the present review, we are going to deal with challenges and perspectives of theragnosis of radionanomedicine.

Radionanomedicine

The success of *in vivo* nanomedicine was received skeptically by the public and even by the experts. This was partly because of the type of components used to make nanoparticles, such as cadmium in quantum dots,[69] but chiefly because of the fear derived from the general ignorance of the *in vivo* characteristics of these new materials, especially when these were to be administered to the human body. Even though the noble metals such as gold[70] or inert silica[71] were used to make nanomaterials for systemic use while expecting the surface of these nanomolecules inert without any surface reactivity, the *in vivo* toxicity of the nanomaterials has been addressed in several reports.[72,73]

Radionanomedicine exploits the traceability of the radiolabeled nanomaterials and decreases the amount of the radiolabeled nanomaterials to a miminum.[74] Only the traceable or deliverable amounts of radiolabeled nanomaterials are needed for systemic use. Because of these advantages, it is highly likely that radionanomedicine will create a breakthrough for the clinical translation of this new discipline of nanomedicine. To prove the feasibility of the easy use of radionanomaterials, the surface modification or labeling of the nanomaterials is the mandatory preliminary step. However, at least one additional step of the labeling and separation of radiolabeled nanomaterials must be taken than the usual modification/labeling steps. Irrespective of the intended purpose, multiplexing the methods of conventional labeling and purification will decrease the recovery of the final product. The discovery of new methods not decreasing the yield after multiple processing steps of labeling or other innovative methods that allow for the simultaneous labeling of all of the final surface-modifiers were highly expected.

The plausible toxicity of nanomedicine has been considered to partly emanate from the constituents of nanomaterials and partly from the surface characteristics of nanoparticles. Furthermore, the permanent residence of the nanoparticles in the mononuclear phagocytic system (MPS) will lead to the synergistic enhancement of the toxicity of the constituents (such as cadmium) and derangement of the MPS cells or immune cells that have phagocytosed the nanoparticles. However, if the nanomaterials are excreted quickly and externally, the toxicity will be minimal and the clinical adaptability to the nanoparticles will be highly increased. To find out whether this is plausible, it is crucial to have an excellent imaging capability, especially with the capacity of quantification of the amount of distributed nanomaterials in the animal or human body. PET or single photon emission computed tomography (SPECT) with or without CT or MRI forms a solution to this challenge. Repetitive quantification of the biodistribution enables the determination of the future applications of newly developed radio-nanomaterials. In addition, a high *in vivo* stability of the radiolabeling is a prerequisite for the quantification of the biodistribution of nanoparticles using their radioactivity.

Surface modification and radiolabeling of nanomaterials

Nanomaterials have vast surfaces compared with those of biomacromolecules or small molecules. However, the majority of the nanomaterials has hydrophobic surfaces after the core synthesis, necessitating the common use of polyethylene glycol (PEG) or natural and synthetic polymers including dextran for making the surface hydrophilic and retaining the material's stability in a biological environment. In addition, ligands and chelators need to be added to the termini of PEGs or the surface of dextran.[75] Ligands should have been chosen from the molecules already known to target the targets that include small molecules or biomacromolecules. The well-known biomacromolecules are either mouse (momab), chimeric (ximab), humanized (zumab), or human (mumab) monoclonal antibodies. Their recently introduced competitors are affibodies,[76] aptamers[77] – either peptide aptamers or nucleic acid aptamers – and the even more recent aptides[78] and avibodies.[79,80] Radiolabeled antibodies have been used for imaging and/or therapy. Both ^{81}Y-labeled ibritumomab tiuxetan (Zevalin®, Biogen Inc., Cambridge, MA, USA), an anti-CD20 monoclonal antibody, and ^{131}I- labeled tositumomab, which is a murine anti-CD20 monoclonal antibody (Bexxar, GlaxoSmithKline, UK), were approved by the FDA for the treatment of non-Hodgkin lymphoma.[82,83] However, ^{131}I-tositumomab was discontinued in February 2014 because of low sales. The effort to develop clinically applicable radiolabeled antibodies continued and in an example report, Hong et al reported a dual labeling method of an anti-CD105 monoclonal antibody with ^{89}Zr and NIRF (near-infrared) dye.[84]

Small moleculear ligands are recognized by their target infrequently, while they sometimes are recognized as opsonins by their target cells or tissues. In that they are recognized more effectively if they are bound to the surface of the nanomaterials, the aptamers or affibodies can be advantageous as ligands. The advantage of these newly introduced aptamers and the likes is derived from the fact that they are produced based on combinatorics, which selects the most desirable macromolecules with optimal affinity and avidity for the target from a large pool of candidates.

Surface modification of nanomaterials with monoclonal antibodies needs the correct combination of the best antibody with the correct direction of labeling. If the binding motif itself is bound to the surface and hidden from the open space, the modified nanomaterials will not bind their target. The most

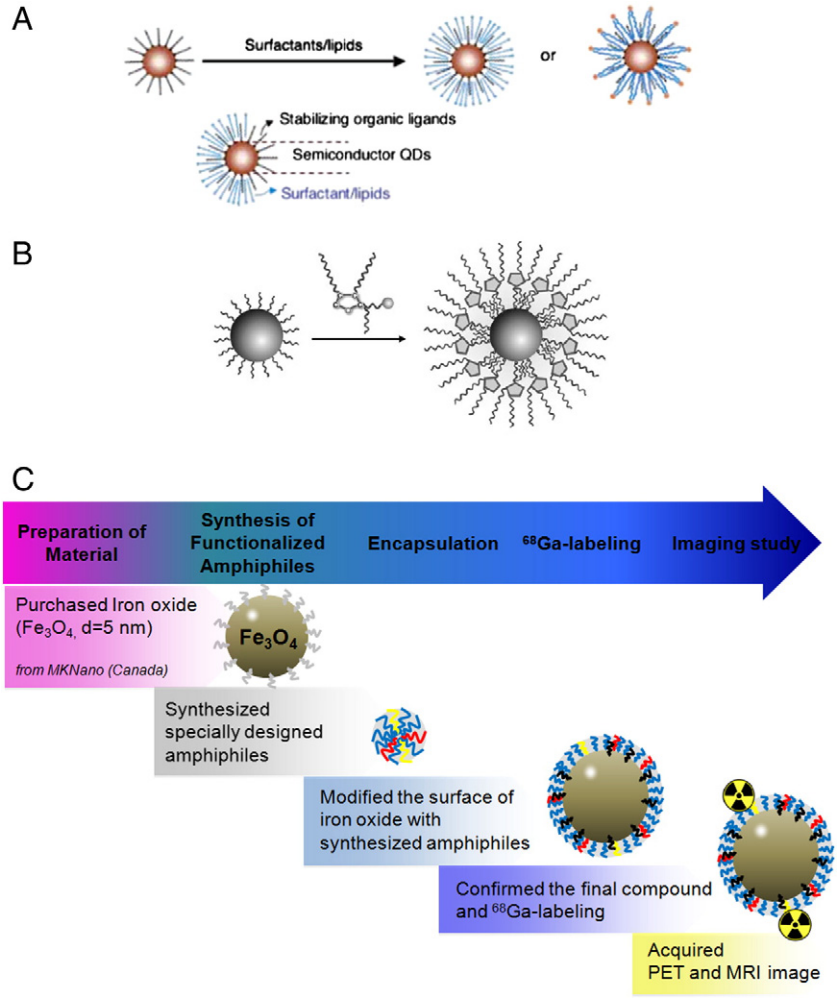

Figure 3. Encapsulation method of nanomaterials using micelles. **(A)** Quantum dots were encapsulated using one-tailed or two-tailed lipids (Reprinted with permission from Ref.[94]). **(B)** Gold, quantum dots, and iron oxide were encapsulated using polyethlyene-glycol (PEG) sorbitan fatty acid esters. (Reprinted with permission from Ref.[95]). **(C)** Iron oxide particles were mixed with multifunctional amphiphiles, vortexed, and separated using size exclusion chromatography. ^{68}Ga was used as radiolabel.

commonly used conjugation method is the coupling of the primary amino-group present on the Fab fragment of the active site of the antibody molecule with the carbodiimide or *N*-hydroxysuccinimide derivatives of the acid-group on the surface of the nanoparticles. Using this method, the antibody-nanoparticle conjugate has a limited number of active groups for efficient targeting.[85,86] To overcome this limitation, site directional conjugation methods have been developed to target the Fc fragment of the antibody through its hydroxyl or disulfide-groups.[85,87]

Some investigators have even attempted to label protein A, which has high affinity for the Fc region of IgG, onto the entire surface of the nanomaterials. Then they further labeled the epitope of protein A with monoclonal antibodies.[88-91] This approach was successful for *in vitro* diagnostics but was not employed for *in vivo* use because of the increased size of the nanoparticles and the fact that the two-step modification process makes the production procedure cumbersome and delivers a low final yield. Hence, a breakthrough in this particular field is necessary.

Hydrophilization of nanomaterials using the micelle encapsulation method was first proposed by Dubertret and colleagues.[92] This method evolved from the use of a two-tailed phospholipid to the use of a one-tailed C-12 alkanethiol.[93] Fan and colleagues introduced microencapsulation and the solvent evaporation method, which was optimized to a quick and simple method[94] (Figure 3, *A*). The Dubertret's group, again using a two-tailed phospholipid, successfully introduced recently functional biomolecules.[96] Wu and colleagues produced micelles by adopting PEG sorbitan fatty acid esters[95] (Figure 3, *B*). Recently, Jeong's group integrated these developments to make a quick and straightforward method of mixing, vortexing, and size exclusion chromatography for producing functionally active multi-specific nanoparticles[50] (Figure 3, *C*). This should be the ultimate solution to the challenge posed in radiolabeling of functional nanomaterials. Jeong ingeniously proposed this one-step method under mild conditions to preserve ligand integrity, which is now called the micelle-encapsulation method.[50] This method was originally used for hydrophilization of quantum dots[92,96] but silica, gold, quantum dots, iron oxide,

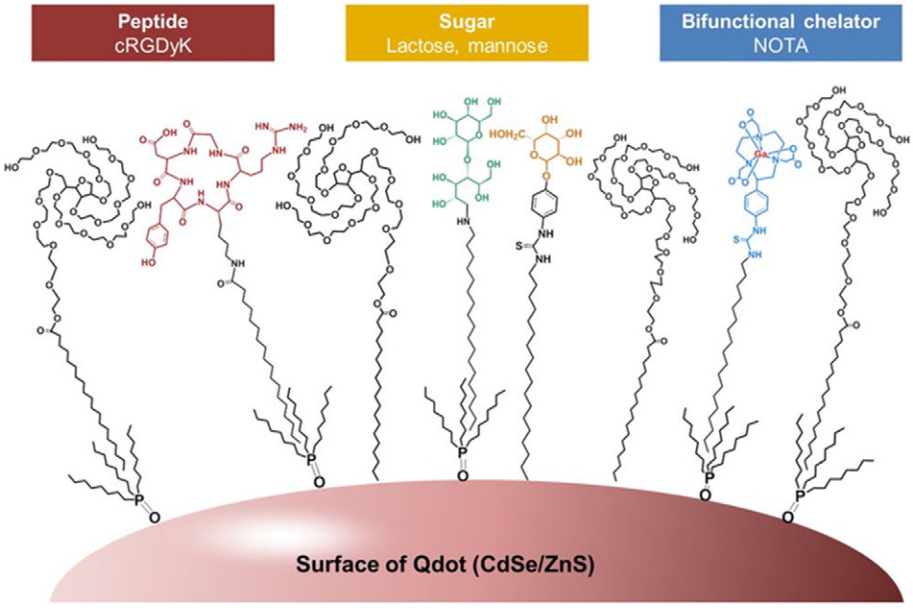

Figure 4. Scheme of the surface modification of nanomaterials (for example, quantum dots) with functional multispecific and multimodal chelator/ligand/Tween60-complex micelles. (Reprinted with permission from Ref.[50]).

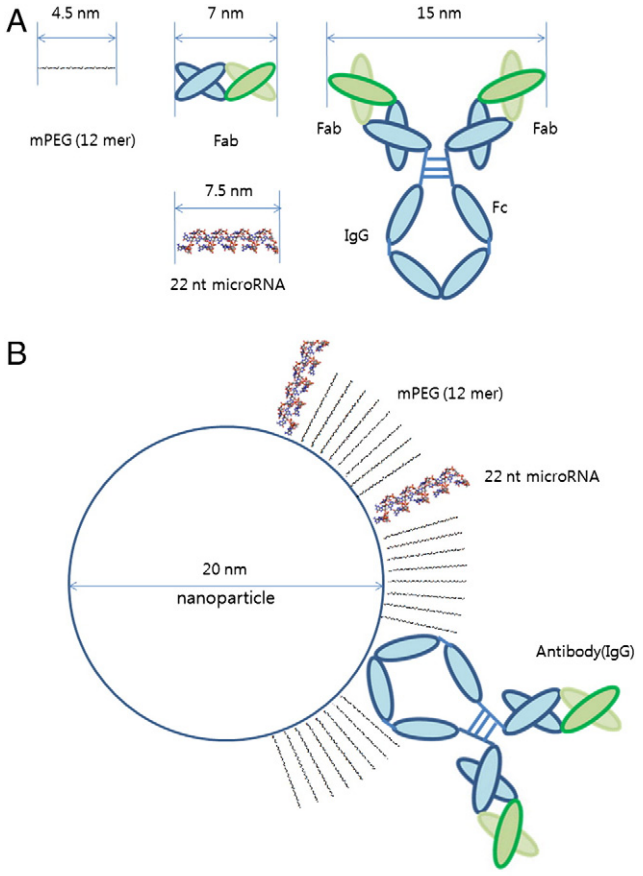

Figure 5. Dimension of an example of a nanomaterial and its surface modifiers such as an antibody, the antibody's Fab fragment, microRNA, or any analogous aptamer or PEG of shorter (12mer) or longer length.

or other hydrophobic nanoparticles were also found to be the appropriate core for encapsulation.[93,95] Jeong's contribution relies on the use of combined multiple amphiphiles with different functional groups simultaneously to achieve surface multifunctionality and hydrophilicity of nanoparticles (Figure 4). In the micelle-encapsulation method, the ligands and the chelator as well as the PEGs are specifically prepared to form a micelle. The micelle in the aqueous phase is then mixed with the nanomaterials in the lipid phase and vortexed to yield the encapsulated nanomaterials. The final multiplexed nanomaterials were purified by size exclusion chromatography. If the small molecules such as mannose, lactose, or cRGD (cyclic Arginine-Glycine-Aspartate) were to be used as ligands, these ligands were covalently bound to the tip of an alkyl chain of optimal length. Using this method, Lee et al labeled QD544T with ^{68}Ga and added functional group of RGD and showed targeted imaging of ^{68}Ga-NOTA-QD655T-RGD in glioma tumor mouse model.[50] Figure 5 depicts the dimension of the modifier ligands and the surface of the nanomaterials if antibodies, aptamer ligands, PEG-chelators, and PEGs were used. Micelle-encapsulation method was employed for iron oxide particles with a diameter of 5 nm,[97,98] upconverting nanoparticles (UCNPs) with a diameter of 50 nm, and other compounds.[99] Surface-enhanced Raman scattering (SERS) dots[100,101] or quantum-dot-embedded silica nanoparticles[102] are other examples of successful encapsulation. If a specific antibody or related peptide/nucleic acid affinity tool is chosen as ligand, chelators and ligands can be used in parallel to surface-label nanomaterials.

The size, the surface charge, and the shape affect the biodistribution of nanomaterials and their combination greatly increases the table of the nanomaterials' *in vivo* characteristics ('periodic table').[103,104] Using the same starting nanomaterials, one can make different surface charges, sizes, and sometimes

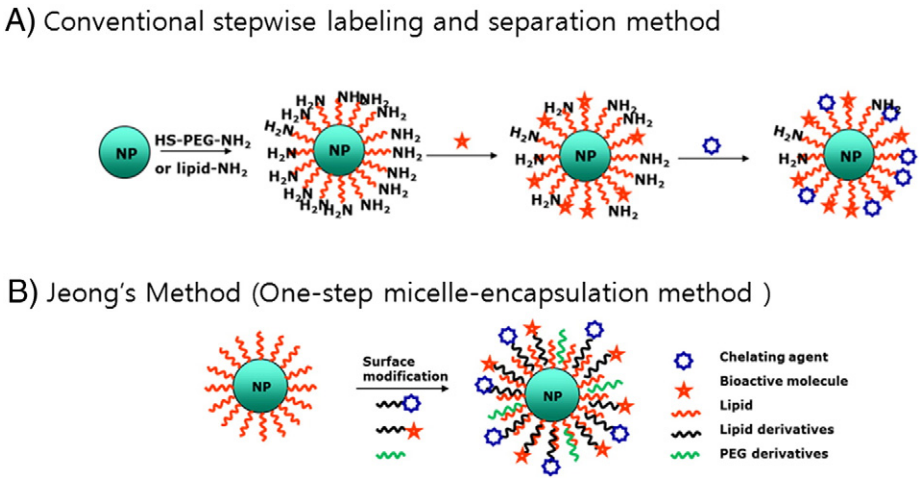

Figure 6. Comparison of the conventional method of surface labeling of multiple functional residues and the one-step micelle-encapsulation method. **(A)** To label the chelator, bioactive molecules (such as targeting ligands) and amphiphiles for hydrophilization (such as PEG), using step-by-step labeling will make the procedure cumbersome with labeling and separation necessary for each step and a low final yield. **(B)** The one-step micelle-encapsulation method allows multispecific micelles (if properly compounded beforehand) to effectively encapsulate any hydrophobic nanomaterials. For both methods, subsequent labeling of the nanomaterials with radioisotopes is needed.

shapes. A different size and surface charge and their combination will lead to different *in vivo* behavior of the nanomaterials. To understand the influence of the differences of these parameters, one needs to prepare nanomaterials of the same size with different surface charges or of the same surface charge with different sizes and examine the biodistribution after systemic delivery. Using conventional labeling and purification methods, the optimization of the synthesis of the specific nanomaterials is difficult or almost impractical. If the one-step method is working while decreasing the burden of the purification step, the investigation time and labor of labeling will decrease considerably and the validity of the periodic table of *in vivo* characteristics will become plausible (Figure 6).

Radionanomedicine might have more barriers to overcome than nanomedicine. If a chelator is added separately, the additional labeling and purification step will result in a decreased recovery and further labeling with a radionuclide will add another step to the process and the radiation-related concerns in processing. One-step labeling of all ligands, the chelator, and PEGs followed by radiolabeling and purification will be an indispensable solution to this problem.

Tracing the *in vivo* distribution of radionanomaterials

Study of the *in vivo* biodistribution of nanomaterials has been performed by exploiting the intrinsic fluorescence or luminescence of nanomaterials or that of nanomaterial surface-labeling dyes and radioisotopes.[104] Fluorescence detection is optimal for the *ex vivo* confirmation of the biodistribution, and for in vivo study fluorescence and luminescence detection is suitable for surface imaging. However, the quantification or depth imaging proved difficult with planar optical imaging. Near infrared (NIR) fluorescence molecular tomography (FMT), enabled depth imaging and quantification of the biodistribution.[105] However, light scattering and tissue absorption resulted in low sensitivity, necessitating the use of an increased amount of fluorescent material (μg) for *in vivo* optical imaging compared with that of radioactive material (ng).[74] The injection of a high dose of an imaging agent can cause a pharmacologic response and might alter the biodistribution.[106] Radiolabeled nanomaterial is the most suitable for imaging and quantification in small animals. Even an application in humans might be, in the long term, possible. Radiolabeled nanomaterials are facile to trace and mimic almost completely the cold (non-radiolabeled) nanomaterials. The chelator, if mixed and merged within the densely packed PEGs on the surface of the nanomaterials, would not make the radiolabeled nanomaterials different from their cold counterparts in terms of the physiological characteristics.

Radionanomaterials can be traced effectively in rodents using small animal SPECT or PET. NOTA can be used as a chelator that can successfully chelate ^{67}Ga and ^{68}Ga, which has a half-life of 3 d and 68 min, respectively.[107] ^{67}Ga can be imaged with small animal SPECT/CT and ^{68}Ga with small animal PET/CT. NOTA could also chelate ^{64}Cu with a resulting half-life of 12.7 h, which was appropriate for the long-term follow-up of the biodistribution of the radiolabeled nanomaterials.[108] For example, chelator-labeled or chelator- free ^{64}Cu-labeled gold nanocages were used to quantify the biodistribution using small animal PET[108,109] (Figure 7, *A* and *B*). In another report, the most commonly used ^{99m}Tc was used to label quantum dots and advantage was taken of the radioisotope's half-life of 6 h to quantify renal excretion.[111] Furthermore, other gamma-ray emitting radioisotopes were used for SPECT imaging[7] (Figure 7, *C* and *D*). Systemically injected radionanomaterial need to avoid phagocytosis by the MPS and immune surveillance to reach the target. Once they reach the tumor target, radionanaomaterials are trapped in the tumor tissue by the enhanced permeability and retention (EPR) effect.[112,113] Further targeting can be achieved by binding the helping ligands to the surface of the nanomaterials for active targeting.[114,115] In a pioneering report by UCLA/Caltech, the biodistribution of a transferrin-liganded nanoparticle labeled with ^{68}Ga was investigated using small animal PET.[116] It was proved that the radiolabeled nanoparticles are first retained

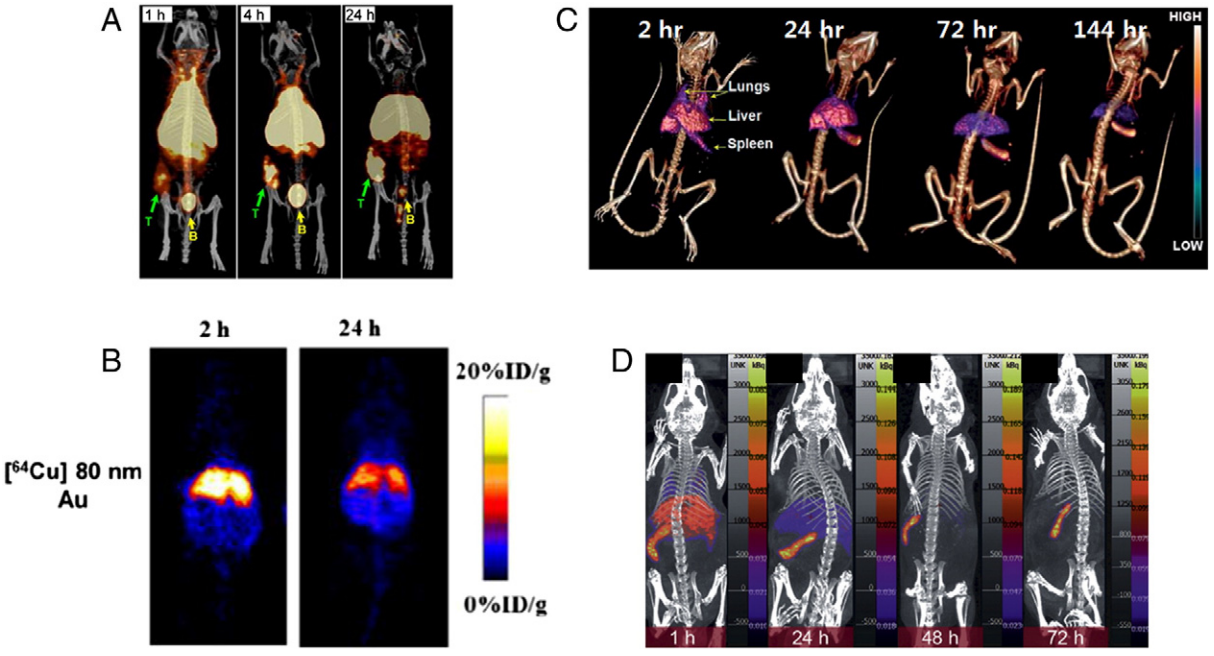

Figure 7. PET/CT and SPECT/CT evaluation of the *in vivo* distribution of radiolabeled nanomaterials. **(A)** Gold nanocage (30 nm in edge length, 60 nm in diameter) was labeled with DOTA that was subsequently chelated with ^{64}C. As observed by PET/CT, after the initial renal excretion, gold particles remained in the liver and spleen. According to the biodistribution data of Ref.,[108] MPS sequestration was the same for small (30 nm) and large (60 nm) nanocages. (Reprinted with permission from Ref.[108]). **(B)** Gold nanomaterials (80 nm) were integrated with ^{64}C. As shown by PET/CT, gold nanoparticles cumulated in the liver and spleen and remained there. (Reprinted with permission from Ref.[109]). **(C)** ^{141}Ce-labeled (145 KeV gamma, T1/2 = 32.5 days) cerium oxide nanoparticles (6 nm) were used for SPECT/CT to reveal the distribution to the liver and spleen. Splenic uptake remained but liver activity faded without showing any intestinal activity, which emphasizes the difference between Kupffer cell and splenic disposal. (Reprinted with permission from Ref.[7]). **(D)** ^{153}Sm-labeled hydroxyapatite nanoparticles (9 nm × 29 nm) were traced for their biodistribution using SPECT/CT, which was enabled by the simultaneous emission of beta and gamma rays by ^{153}Sm. After the initial liver and spleen uptake, only the splenic uptake remained active at 72 h after injection. (Reprinted with permission from Ref.[110]).

in the tumor tissue by EPR, with transferrin further retaining those particles *in situ*. Tracer kinetic modeling enabled this discovery. In this experiment, siRNA was used as a therapeutic.[116]

Because of their relatively long half-life, only ^{67}Ga, ^{64}Cu, or ^{89}Zr enable the localization, excretion, and behavior of the radiolabeled nanomaterials days after their administration. If the excretion of the radiolabeled nanomaterial will prove to be complete after several days, concerns about the possible *in vivo* toxicity might be diminished. In particular, the use of high pharmacological amounts of nanomaterials or phobia of the persistent residence of nanomaterials in various organs could be avoided. The radiolabeled nanomaterials will help decrease the total amount of nanomaterials to be injected.

^{177}Lu was used as the therapeutic radionuclide[61] in the octreotide used as the ligand for neuro-endocrine tumors, which was chelated by DOTA bound covalently to the octreotide. Fortunately, the DOTA-octreotide complex acted like the unlabeled octreotide as was the case with ^{177}Lu-labeled DOTA-octreotide. In this case, ^{177}Lu emits 208 KeV gamma rays with 11% of the entire emission. SPECT/CT could visualize whether ^{177}Lu was taken up within the metastatic tumors and even quantify the remaining tumors. ^{177}Lu also emits 0.498 MeV beta rays, which are suitable for the destruction of the targeted tumors. A major limitation of the treatment using ^{177}Lu-labeled DOTA-octreotide is the nephrotoxicity due to high renal uptake. To reduce nephrotoxicity, ^{177}Lu-DOTA-octreotide could be conjugated to nanoparticles. Arora et al reported that nanoparticle-conjugated ^{177}Lu-DOTA-octreotide showed lower renal uptake than ^{177}Lu-DOTA-octreotide.[117] When octreotide is bound onto the surface of the nanomaterials, care has to be taken to maintain the binding affinity of the octreotide-bound nanomaterials to the octreotide receptors. Surface plasmon response (SPR) analysis could be used to measure the binding affinity of octreotide-bound nanomaterials. A difference can exist between naïve octreotide and octreotide-bound nanomaterials. However, this difference has to be limited for octreotide-bound nanomaterials to be used for targeted delivery and imaging. Instead of octreotide, an affibody, aptamer, or aptide can be used to modify the nanomaterial surface. An affibody or aptamer can have a binding motif, which should be still be available for binding to the target after concomitant surface modification of the nanoparticles.

For ^{89}Zr, desferrioxamine (DFO) is used for chelation of this radionuclide.[60] ^{89}Zr chemistry is still in its infancy, but the chelator can label the surface of micro-encapsulated nanomaterials. For therapeutic purposes, ^{90}Y can be used as the beta-ray emitter. ^{90}Y is produced both in a nuclear reactor or generator. ^{90}Y emits only beta rays of 2.28 MeV. The absence of the gamma ray emission makes the theragnostic application of ^{90}Y difficult. The

same chelators such as DOTA or NOTA can be used for labeling ^{90}Y to nanomaterials.

Degradation and excretion of radionanomaterials evaluated by molecular imaging

Nanomaterials, either cold or radiolabeled, will form a cluster of the larger particles covered by corona proteins once administered into the intravascular compartments.[118,119] Corona proteins are classified into soft and hard proteins, of which the soft ones could be easily detached from the corona-nanoparticle complexes, whereas the hard corona proteins were fixed firmly to the nanoparticle.[120] Whether the radionuclides of the radiolabeled nanomaterials are stable in the blood should be examined in detail using radio-thin layer chromatography (radioTLC) or imaging studies. However, chelation of the radioactive metals by DTPA, DOTA, or NOTA has been determined to be quite stable in the case of small molecules and biomacromolecules.[56-59]

The surface ligands of the nanomaterials should remain stably attached, at least until the radiolabeled nanomaterials have reached their targets. Degradation of the radiolabeled ligands will make the biodsitribution by the nuclear imaging not exactly represent the materials' distribution.[109] The pitfalls of the 'tracer technology' become apparent compared with when the original material is examined. When radiolabeled nanomaterials are used to investigate degradation and excretion of large nanomaterials, if the radiolabel is detached rapidly, the examining tracer's whereabouts does not represent those of the authentic nanomaterials. Nanomaterials can lose their surface modifiers, especially the large ligands such as monoclonal antibodies, targeting peptides, and aptamers, and other small ligands such as cRGD[80] or mannose.[81,121] Recently, a strategy of intrinsic radiolabeling of nanoparticle core has emerged, which facilitated labeling quantum dots with ^{111}In[122] or gold dots with ^{198}Au.[123-125] When one uses surface-radiolabeling, the stability of the chelating radioisotopes or the comparison of the radioisotope-chelator complex and radioisotope-chelator-nanomaterial complex should have been performed.[74,126]

The excretion of the radiolabeled nanomaterials could be tested effectively with small animal PET (Figure 8). UCNPs with a radiolabeled surface could be traced for their excretion.[104] Using upconversion luminance imaging and small animal PET the excretion through the hepatobiliary route could be precisely shown and even the fecal excretion could be confirmed by imaging the excreta. Electron microscopy could visualize the excretion of the nanoparticles through sinusoid, hepatocyte, and bile canaliculi to the intestines. Small animal PET could visualize the collection of excreted radioactivity in the gall bladder and the ejection into the intestines (Figure 9).

Radiolabeled nanomaterials with a size of less than 8 nm were expected to be excreted via the kidneys.[104,111,131] However, the size-dependence of nanomaterial excretion is somewhat ambiguous mainly because the hepatobiliary excretion of larger nanomaterials is not well characterized[132] (Figure 8). The renal excretion is much faster than the hepatobiliary route. The charge and shape as well as the size were reported to be important factors to determine the renal excretion.[104,123,133] The hydrophilicity seems to affect the aggregation of nanomaterials injected into the systemic route, resulting in distribution to the lungs by blocking the capillaries.[123,124,126,134] Once the nanomaterials have passed the pulmonary capillaries, if they were taken up by the liver, they have long been considered to be taken up in the MPS of the liver and spleen and, finally, in the bone marrow[110,135-138] (Figure 7). However, the surface characteristics seem to determine the excretability of nanomaterials through the hepatobiliary system, which is not well understood yet.[125-127] If nanomaterials are encapsulated and their excretion will be traced, as the radiolabeled nanoparticles using micelle-encapsulation methods mimic micelles, the excretion pattern should be compared with that of micelles or liposomes.[128-130,139]

Both renal and hepatobiliary pathways form the main excretion route for clearing of the nanomaterials from the body. Radiolabeled nanomaterials can be considered safe for *in vivo* use if these nanomaterials are excreted completely within a sufficient time. After 18-24 h, about one-half of the radiolabeled nanomaterials are excreted, necessitating a third and fourth day of imaging. ^{89}Zr with a half-life of 78.4 h might be more suitable than ^{64}Cu. Liu et al reported a rapid hepatic excretion of hydroxyapatite nanorods within 72 h. However, the excretion pathway was not clear because a negligible amount of nanoparticle was present in the urine and the intestines both in the *in vivo* imaging and *ex vivo* biodistribution study[110] (Figure 7, *D*). Xiao et al reported a higher tumor targeting using micelles while showing hepatobiliary excretion[128] (Figure 8, *B*). Rangger et al also reported a rapid hepatic excretion of multifunctional liposomal nanoparticles[129] (Figure 8, *C*). In tumor-bearing nude mice, small animal SPECT/CT revealed the rapid excretion of ^{111}In-labeled liposomal nanoparticles from the liver to the intestines. Currently, the chemistry of chelating and modifying the surface of the nanomaterials with ^{89}Zr and desferrioxamine or others is under investigation.

Predicting the immune responses to radiolabeled nanomaterials beyond physiological monitoring

Either nanomaterials or radiolabeled nanomaterials evoke bodily immune responses upon administration. Pharmacologic amounts of nanomaterials produce pharmacological effects and the constituents of the nanomaterials either in the core or on the surface will be the determinants of these effects. However, the bodily responses to the systemically administered nanomaterials or radiolabeled nanomaterials are also processed from an immunological perspective. Complement activation-related pseudoallergy is the most famous immunological response to nanomaterials such as liposomes.[140] This reaction arises even at the first encounter, unlike the IgE-mediated anaphylaxis reaction. Complement activation precedes mediator releases such as anaphylatoxin, perforin, or opsonin and their following lipid mediators.

The innate immunity was long suspected to defend the intrusion of silica or other hydrophobic materials.[141,142] The immune surveillance system detects the patterns mimicking

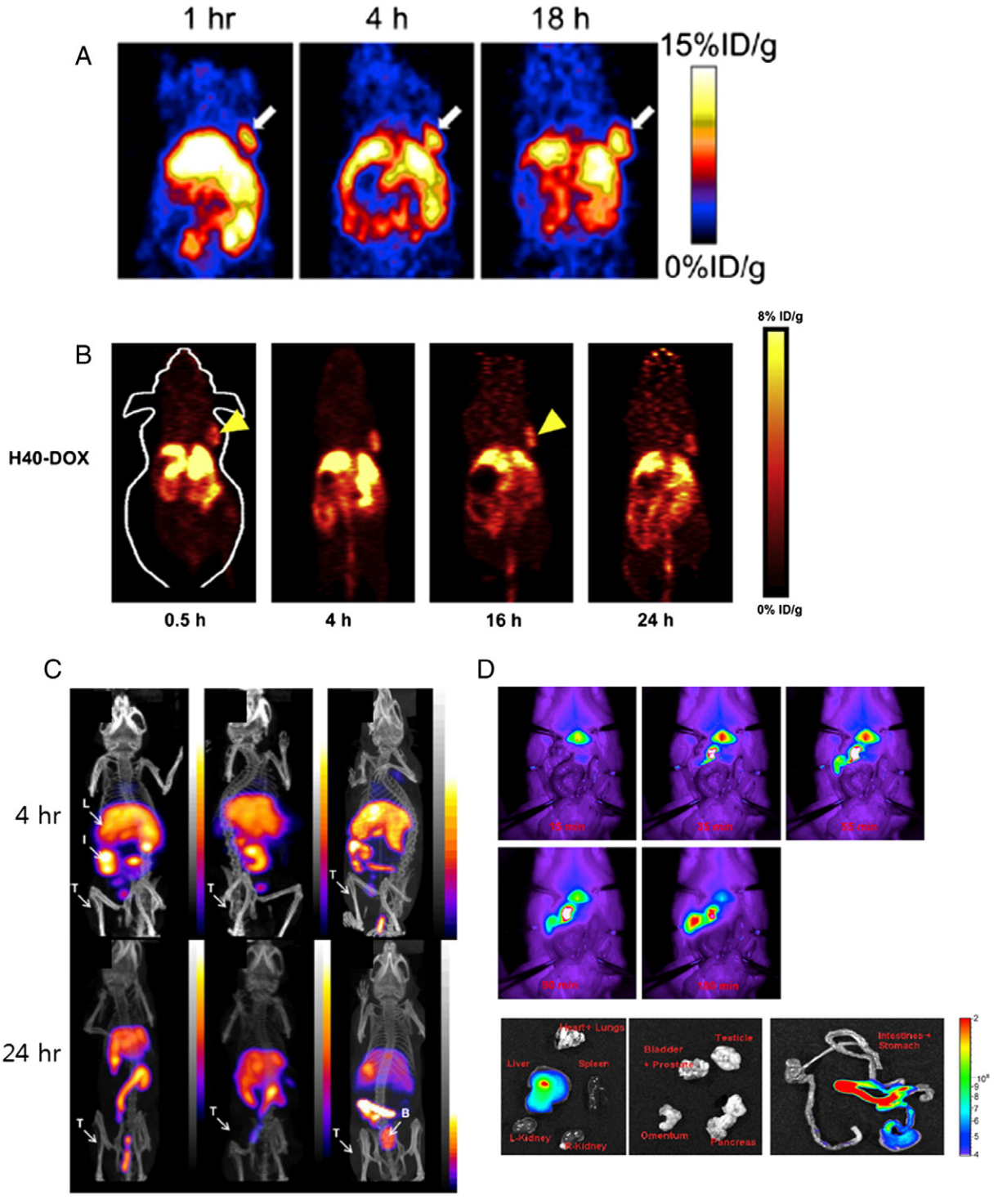

Figure 8. The degradation and excretion of radiolabeled nanomaterial evaluated by PET/CT or SPECT/CT. **(A)** Iron oxide nanoparticles (15 nm) were surface-modified using human serum albumin (29 nm after labeling) and labeled with DOTA and ^{64}C. Once injected *in vivo*, beside tumor uptake, the hepatic excretion was ascertained by PET. (Reprinted with permission from Ref.[127]). **(B)** Micelles (65 nm) encapsulating H40 (a hyperbranched aliphatic polyester) were labeled with NOTA and^{110}C. Encapsulated H40 nanoparticles were excreted via the hepatobiliary pathway. (Reprinted with permission from Ref.[128]). **(C)** Targeted or non-targeted liposomes (110-131 nm) labeled with ^{111}In were injected and examined for their degradation and excretion. The hepatic and intestinal excretion was observed. (Reprinted with permission from Ref.[129]). **(D)** Silica nanoparticles (50-100 nm) labeled with indocyanin green were traced for their excretion and showed a rapid hepatobiliary excretion. (Reprinted with permission from Ref.[130]).

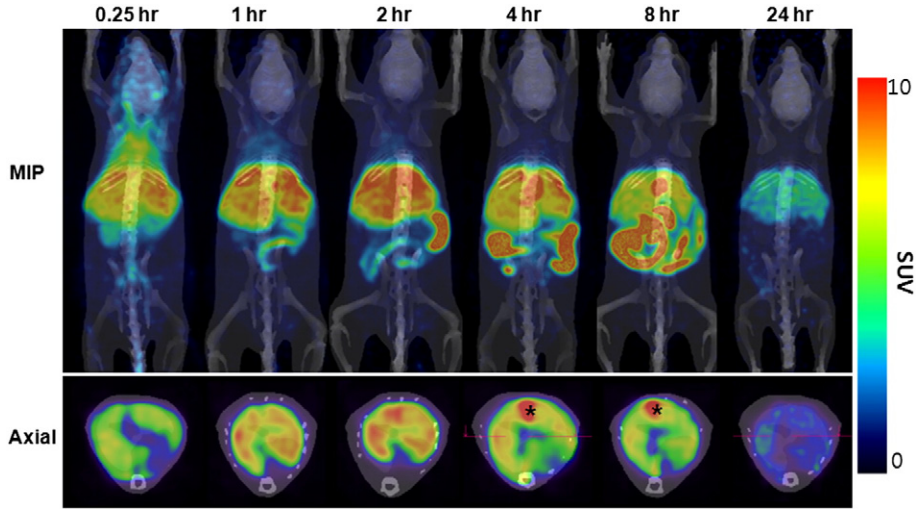

Figure 9. Upconversion nanoparticle (UCNP) encapsulated with micelles containing PEG (Tween-60)/chelator and ^{64}Cu. Using PET/CT, the uptake of radiolabeled UCNPs by the hepatocytes and the excretion via the biliary routes to the intestines with expulsion as feces was imaged. The arrow points to the gallbladder.

lipopolysaccharides, viral capsids, or bacterial exosomes. Silica and other hydrophobic nanoparticles stimulate toll-like receptors (TLRs)[141-148] and NOD-like receptors on the cellular membranes and on the inside of the cells, which leads to the activation of the inflammasome.[149,150] Nanoparticle hydrophobicity[151] and shape[75,152] were the major determinants in the immune and inflammatory responses to gold nanoparticles and carbon nanotubes, respectively. Mizrahy et al reported that hyaluronan-coated nanoparticle does not induce an immune response *in vitro*.[153] Surface modification can change the immune response to the administered nanomaterials and should be the focus of further study. The adaptive immunity consisting of humoral and cellular responses can be induced but this is not entirely clear yet.[154]

The prediction of immune responses to nanomaterials either by themselves or when radiolabeled is difficult,[155] however, radiolabeling would not elicit an additional immune reaction to the original nanoparticles. Rather, PEGylation and the concomitant modification of the surface of the nanomaterials can change the response of the immune system and can result in the silencing of the immune response.[156] This was first called the "stealth effect". However, several reports have demonstrated that the PEG itself elicited an IgM response[157]; nevertheless, this is open to opposing interpretations.[156]

Elucidation of the *in vivo* systemic immune responses to the nanomaterials needs concomitant understanding of the physiological outcomes of the disposal of systemically injected nanomaterials, and, likewise, of the immune responses.[155] The MPS of the liver, spleen, and bone marrow are considered to be the main disposal sites of the nanomaterials, although the difference between these sites, especially between the liver and the spleen, needs further attention. Investigating how the spleen filters foreign nanomaterials, Discher's group inhibited the splenic macrophage capture, while surface-bound self-peptides could confer the nanoparticles to escape from the foreign substance recognition mechanism.[158,159] The hepatic uptake of nanomaterials is more complex in that both Kupffer cells and hepatocytes clear the nanomaterials from the circulation. Sometimes, the hepatic uptake disappears but splenic uptake continues, and the disappearance of the initial hepatic uptake should be considered to be due to hepatobiliary excretion.[160,161] Bergen et al already attempted to label nanomaterials with galactose to enhance their hepatocyte uptake and biliary excretion.[162]

From the viewpoint of targeted delivery, MPS clearance of nanomaterials administered *in vivo* is considered as nonspecific uptake and surface coating was carried out to decrease this uptake.[163] From the viewpoint of immunotoxicicity, nanomaterials elicit immune responses of various types such as complement activation, innate and adaptive immune responses, and possibly tolerance or immune enhancement, all of which are associated with systemic hemodynamic responses or localized inflammation. Among them, the immunomodulatory properties of nanomaterials were exploited to potentiate the immune response and immunotherapy.[164] In terms of toxicity, the acute or long-term localization of administered nanomaterials *in vivo* was questioned and the biodistribution was scrutinized. Nonetheless, it is still not clear whether the nanomaterials themselves, or the dosing effect, surface-bound small or macromolecules, immune/inflammatory response to these surface-bound ligands, hydrophobic/hydrophilic surface characteristics, or electric charges, are the critical determinants of the biomedical hazard to the recipient.[165,166] Surface modification of nanomaterials should not be considered equal even though all were known to be PEGylated. Surface hydrophilicity or corona modification varies from one nanomaterial to another; this is reminiscent of the decade-long pursuit of understanding the exact nature of PEGylated liposome clearance[167,168] and the recent micelle distribution and clearance. Radiolabeled nanomaterials will enable us, with their imaging capability, to differentiate between the individual determinants of the bodily responses and of the *in vivo* fate of newly developed nanomaterials.

By injection of radionanomaterial to the human body, toxicity can be caused by not only nanomaterial itself but also radiation exposure. However, we could not find any study to evaluate

thoroughly the dosimetry after theragnostic use of radionanomaterials. If we are going to apply a new radionanomaterial for possible human use, we also need do the dosimetry studies in the same way as we did when we had developed therapeutic small-molecular radiotracers.[169,170]

Molecular theragnosis and radionanomedicine

Molecular targets are mainly expressed on the cell surface. In tumors, they reside on the cellular membranes; hence, the EPR effects of nanomaterials were expected to result in tumor targeting. Passive targeting was the primary cause of nanomaterials to reach their target. Active targeting can further help the targeted delivery by enhancing selective retention. However, before the development of a strategy for active targeting, we need to understand first the *in vivo* distribution and localization of nanomaterials after systemic administration. Radiolabeling will make tracing radiolabeled nanomaterials *in vivo* straightforward as well as the excretory pattern from the body and the ratio of the MPS uptake per total injected amount of radio-labeled nanomaterial.[71]

Another advantage of using radiolabeled nanomaterials for *in vivo* theragnosis is that the amount of nanomaterials for use *in vivo* can be decreased as low as possible, eliminating the concerns about the possible hazards of pharmacologic amount of nanomaterials administered to animals and humans. This is the trace technology behind radionanomedicine and will sure help the progress of the translation of nanomedicine to the clinics. Once the gross physiology and the immune responses are well understood in small animals using small animal SPECT/CT or small animal PET/CT devices, we might be able to understand the intracellular location of nanomaterials after endocytosis. In addition to the surface molecules, if the intracellular molecules are chosen as targets, the perspectives or premises of the molecular theragnostics will likely be expanded.

Acknowledgment

This study was supported by a grant from the Korea Healthcare technology R&D Project, Ministry for Health, Welfare & Family Affairs, Republic of Korea (Nanobioimaging project : HI13C-1299-020013), the BK21plus Research Project, and the future-based technology development program of the NRF funded by the MEST (20100028755).

References

1. Kagan VE, Bayir H, Shvedova AA. Nanomedicine and nanotoxicology: two sides of the same coin. *Nanomedicine* 2005;**1**(4):313-6.
2. Garnett MC, Kallinteri P. Nanomedicines and nanotoxicology: some physiological principles. *Occup Med (Lond)* 2006;**56**(5):307-11.
3. Maurer-Jones MA, Bantz KC, Love SA, Marquis BJ, Haynes CL. Toxicity of therapeutic nanoparticles. *Nanomedicine (Lond)* 2009;**4**(2):219-41.
4. Donaldson K, Aitken R, Tran L, Stone V, Duffin R, Forrest G. Carbon nanotubes: a review of their properties in relation to pulmonary toxicology and workplace safety. *Toxicol Sci* 2006;**92**(1):5-22.
5. Sun G, Xu J, Hagooly A, Rossin R, Li Z, Moore DA, et al. Strategies for optimized radiolabeling of nanoparticles for in vivo pet imaging. *Adv Mater* 2007;**19**(20):3157-62.
6. Sun M, Hoffman D, Sundaresan G, Yang L, Lamichhane N, Zweit J. Synthesis and characterization of intrinsically radiolabeled quantum dots for bimodal detection. *Am J Nucl Med Mol Imaging* 2012;**2**(2):122-35.
7. Yang L, Sundaresan G, Sun M, Jose P, Hoffman D, McDonagh PR, et al. Intrinsically radiolabeled multifunctional cerium oxide nanoparticles for in vivo studies. *J Mat Chem B* 2013;**1**(10):1421-31.
8. Zhou M, Zhang R, Huang M, Lu W, Song S, Melancon MP, et al. A chelator-free multifunctional [^{64}Cu]CuS nanoparticle platform for simultaneous micro-PET/CT imaging and photothermal ablation therapy. *J Am Chem Soc* 2010;**132**(43):15351-8.
9. Wong RM, Gilbert DA, Liu K, Louie AY. Rapid size-controlled synthesis of dextran-coated, ^{64}Cu-doped iron oxide nanoparticles. *ACS Nano* 2012;**6**(4):3461-7.
10. Zhao Y, Sultan D, Detering L, Cho S, Sun G, Pierce R, et al. Copper-64-alloyed gold nanoparticles for cancer imaging: improved radiolabel stability and diagnostic accuracy. *Angew Chem Int Ed Engl* 2014;**53**(1):156-9.
11. Lin X, Xie J, Niu G, Zhang F, Gao H, Yang M, et al. Chimeric ferritin nanocages for multiple function loading and multimodal imaging. *Nano Lett* 2011;**11**(2):814-9.
12. Liu TW, MacDonald TD, Shi J, Wilson BC, Zheng G. Intrinsically copper-64-labeled organic nanoparticles as radiotracers. *Angew Chem Int Ed Engl* 2012;**51**(52):13128-31.
13. Katti KV, Kannan R, Katti K, Kattumori V, Pandrapraganda R, Rahing V, et al. Hybrid gold nanoparticles in molecular imaging and radiotherapy. *Czechoslov J Phys* 2006;**56**(1):D23-34.
14. Khan MK, Minc LD, Nigavekar SS, Kariapper MS, Nair BM, Schipper M, et al. Fabrication of ^{198}Au radioactive composite nanodevices and their use for nanobrachytherapy. *Nanomedicine (Lond)* 2008;**4**(1):57-69.
15. Chanda N, Kan P, Watkinson LD, Shukla R, Zambre A, Carmack TL, et al. Radioactive gold nanoparticles in cancer therapy: therapeutic efficacy studies of GA-^{198}AuNP nanoconstruct in prostate tumor-bearing mice. *Nanomedicine (Lond)* 2010;**6**(2):201-9.
16. Shukla R, Chanda N, Zambre A, Upendran A, Katti K, Kulkarni RR, et al. Laminin receptor specific therapeutic gold nanoparticles (^{198}AuNP-EGCg) show efficacy in treating prostate cancer. *Proc Natl Acad Sci U S A* 2012;**109**(31):12426-31.
17. Zhou C, Hao G, Thomas P, Liu J, Yu M, Sun S, et al. Near-infrared emitting radioactive gold nanoparticles with molecular pharmacokinetics. *Angew Chem Int Ed Engl* 2012;**51**(40):10118-22.
18. Wang Y, Liu Y, Luehmann H, Xia X, Wan D, Cutler C, et al. Radioluminescent gold nanocages with controlled radioactivity for real-time in vivo imaging. *Nano Lett* 2013;**13**(2):581-5.
19. Yang Y, Sun Y, Cao T, Peng J, Liu Y, Wu Y, et al. Hydrothermal synthesis of NaLuF4:153Sm, Yb, Tm nanoparticles and their application in dual-modality upconversion luminescence and SPECT bioimaging. *Biomaterials* 2013;**34**(3):774-83.
20. Sun Y, Zhu X, Peng J, Li F. Core-shell lanthanide upconversion nanophosphors as four-modal probes for tumor angiogenesis imaging. *ACS Nano* 2013;**7**(12):11290-300.
21. Zeng J, Jia B, Qiao R, Wang C, Jing L, Wang F, et al. In situ ^{111}In-doping for achieving biocompatible and non-leachable ^{111}In-labeled Fe3O4 nanoparticles. *Chem Commun (Camb)* 2014;**50**(17):2170-2.
22. Sun Y, Yu M, Liang S, Zhang Y, Li C, Mou T, et al. Fluorine-18 labeled rare-earth nanoparticles for positron emission tomography (PET) imaging of sentinel lymph node. *Biomaterials* 2011;**32**(11):2999-3007.
23. Liu Q, Sun Y, Li C, Zhou J, Yang T, Zhang X, et al. ^{18}F-Labeled magnetic-upconversion nanophosphors via rare-Earth cation-assisted ligand assembly. *ACS Nano* 2011;**5**(4):3146-57.
24. Chen F, Ellison PA, Lewis CM, Hong H, Zhang Y, Shi S, et al. Chelator-free synthesis of a dual-modality PET/MRI agent. *Angew Chem Int Ed Engl* 2013;**52**(50):13319-23.

25. Chakravarty R, Valdovinos HF, Chen F, Lewis CM, Ellison PA, Luo H, et al. Intrinsically germanium-69-labeled iron oxide nanoparticles: synthesis and in-vivo dual-modality PET/MR imaging. *Adv Mater* 2014;**26**(30):5119-23.
26. Morales-Avila E, Ferro-Flores G, Ocampo-Garcia BE, De Leon-Rodriguez LM, Santos-Cuevas CL, Garcia-Becerra R, et al. Multimeric system of 99mTc-labeled gold nanoparticles conjugated to c[RGDfK(C)] for molecular imaging of tumor alpha(v)beta(3) expression. *Bioconjug Chem* 2011;**22**(5):913-22.
27. Mendoza-Sanchez AN, Ferro-Flores G, Ocampo-Garcia BE, Morales-Avila E, de MRF, De Leon-Rodriguez LM, et al. Lys3-bombesin conjugated to ^{99m}Tc-labelled gold nanoparticles for in vivo gastrin releasing peptide-receptor imaging. *J Biomed Nanotechnol* 2010;**6**(4):375-84.
28. Ocampo-Garcia BE, Ramirez Fde M, Ferro-Flores G, De Leon-Rodriguez LM, Santos-Cuevas CL, Morales-Avila E, et al. ^{99m}Tc-labelled gold nanoparticles capped with HYNIC-peptide/mannose for sentinel lymph node detection. *Nucl Med Biol* 2011;**38**(1):1-11.
29. Zhang G, Yang Z, Lu W, Zhang R, Huang Q, Tian M, et al. Influence of anchoring ligands and particle size on the colloidal stability and in vivo biodistribution of polyethylene glycol-coated gold nanoparticles in tumor-xenografted mice. *Biomaterials* 2009;**30**(10):1928-36.
30. Torres Martin de Rosales R, Tavare R, Glaria A, Varma G, Protti A, Blower PJ. ^{99m}Tc-bisphosphonate-iron oxide nanoparticle conjugates for dual-modality biomedical imaging. *Bioconjug Chem* 2011;**22**(3):455-65.
31. Cai W, Chen K, Li ZB, Gambhir SS, Chen X. Dual-function probe for PET and near-infrared fluorescence imaging of tumor vasculature. *J Nucl Med* 2007;**48**(11):1862-70.
32. Chen K, Conti PS. Target-specific delivery of peptide-based probes for PET imaging. *Adv Drug Deliv Rev* 2010;**62**(11):1005-22.
33. Xie H, Diagaradjane P, Deorukhkar AA, Goins B, Bao A, Phillips WT, et al. Integrin alphavbeta3-targeted gold nanoshells augment tumor vasculature-specific imaging and therapy. *Int J Nanomedicine* 2011;**6**:259-69.
34. Lee HY, Li Z, Chen K, Hsu AR, Xu C, Xie J, et al. PET/MRI dual-modality tumor imaging using arginine-glycine-aspartic (RGD)-conjugated radiolabeled iron oxide nanoparticles. *J Nucl Med* 2008;**49**(8):1371-9.
35. Jarrett BR, Gustafsson B, Kukis DL, Louie AY. Synthesis of ^{64}Cu-labeled magnetic nanoparticles for multimodal imaging. *Bioconjug Chem* 2008;**19**(7):1496-504.
36. Glaus C, Rossin R, Welch MJ, Bao G. In vivo evaluation of ^{64}Cu-labeled magnetic nanoparticles as a dual-modality PET/MR imaging agent. *Bioconjug Chem* 2010;**21**(4):715-22.
37. Liu Z, Cai W, He L, Nakayama N, Chen K, Sun X, et al. In vivo biodistribution and highly efficient tumour targeting of carbon nanotubes in mice. *Nat Nanotechnol* 2007;**2**(1):47-52.
38. Petersen AL, Binderup T, Rasmussen P, Henriksen JR, Elema DR, Kjaer A, et al. ^{64}Cu loaded liposomes as positron emission tomography imaging agents. *Biomaterials* 2011;**32**(9):2334-41.
39. Qingnuan L, Yan X, Xiaodong Z, Ruili L, Qieqie D, Xiaoguang S, et al. Preparation of ^{99m}Tc-C(60)(OH)(x) and its biodistribution studies. *Nucl Med Biol* 2002;**29**(6):707-10.
40. Guo J, Zhang X, Li Q, Li W. Biodistribution of functionalized multiwall carbon nanotubes in mice. *Nucl Med Biol* 2007;**34**(5):579-83.
41. Singh R, Pantarotto D, Lacerda L, Pastorin G, Klumpp C, Prato M, et al. Tissue biodistribution and blood clearance rates of intravenously administered carbon nanotube radiotracers. *Proc Natl Acad Sci U S A* 2006;**103**(9):3357-62.
42. McDevitt MR, Chattopadhyay D, Kappel BJ, Jaggi JS, Schiffman SR, Antczak C, et al. Tumor targeting with antibody-functionalized, radiolabeled carbon nanotubes. *J Nucl Med* 2007;**48**(7):1180-9.
43. Zhang R, Lu W, Wen X, Huang M, Zhou M, Liang D, et al. Annexin A5-conjugated polymeric micelles for dual SPECT and optical detection of apoptosis. *J Nucl Med* 2011;**52**(6):958-64.
44. Park JC, Yu MK, An GI, Park SI, Oh J, Kim HJ, et al. Facile preparation of a hybrid nanoprobe for triple-modality optical/PET/MR imaging. *Small* 2010;**6**(24):2863-8.
45. Lee J, Lee TS, Ryu J, Hong S, Kang M, Im K, et al. RGD peptide-conjugated multimodal NaGdF4:Yb3+/Er3+ nanophosphors for upconversion luminescence, MR, and PET imaging of tumor angiogenesis. *J Nucl Med* 2013;**54**(1):96-103.
46. Cao J, Wang Y, Yu J, Xia J, Zhang C, Yin D, et al. Preparation and radiolabeling of surface-modified magnetic nanoparticles with rhenium-188 for magnetic targeted radiotherapy. *J Magn Magn Mater* 2004;**277**(1-2):165-74.
47. Liang S, Wang Y, Yu J, Zhang C, Xia J, Yin D. Surface modified superparamagnetic iron oxide nanoparticles: as a new carrier for biomagnetically targeted therapy. *J Mater Sci Mater Med* 2007;**18**(12):2297-302.
48. Chang YJ, Chang CH, Chang TJ, Yu CY, Chen LC, Jan ML, et al. Biodistribution, pharmacokinetics and microSPECT/CT imaging of ^{188}Re-bMEDA-liposome in a C26 murine colon carcinoma solid tumor animal model. *Anticancer Res* 2007;**27**(4B):2217-25.
49. Luna-Gutiérrez M, Ferro-Flores G, Ocampo-García BE, Santos-Cuevas CL, Jiménez-Mancilla N, De León-Rodríguez LM, et al. A therapeutic system of ^{177}lu-labeled gold nanoparticles-RGD internalized in breast cancer cells. *J Mex Chem Soc* 2013;**57**:212-9.
50. Lee YK, Jeong JM, Hoigebazar L, Yang BY, Lee YS, Lee BC, et al. Nanoparticles modified by encapsulation of ligands with a long alkyl chain to affect multispecific and multimodal imaging. *J Nucl Med* 2012;**53**(9):1462-70.
51. Hwang DW, Ko HY, Lee JH, Kang H, Ryu SH, Song IC, et al. A nucleolin-targeted multimodal nanoparticle imaging probe for tracking cancer cells using an aptamer. *J Nucl Med* 2010;**51**(1):98-105.
52. Goel S, Chen F, Ehlerding EB, Cai W. Intrinsically radiolabeled nanoparticles: an emerging paradigm. *Small* 2014;**10**(19):3825-30.
53. Xing Y, Zhao J, Conti PS, Chen K. Radiolabeled nanoparticles for multimodality tumor imaging. *Theranostics* 2014;**4**(3):290-306.
54. Enrique Morales-Avila GF-F, Ocampo-García Blanca E, Ramírez Flor de María. Radiolabeled nanoparticles for molecular imaging. In: Schaller B, editor. *InTech*; 2012.
55. Wadas TJ, Wong EH, Weisman GR, Anderson CJ. Coordinating radiometals of copper, gallium, indium, yttrium, and zirconium for PET and SPECT imaging of disease. *Chem Rev* 2010;**110**(5):2858-902.
56. Lee YS. Radiopharmaceutical chemistry. In: Kim EELD, Tateishi U, Baum R, editors. *Handbook of nuclear medicine and molecular imaging*. NJ, USA: World Scientific Publishing Co. Pte. Ltd.; 2012. p. 21-51.
57. Velikyan I. Prospective of ^{68}Ga-radiopharmaceutical development. *Theranostics* 2013;**4**(1):47-80.
58. Niccoli Asabella A, Cascini GL, Altini C, Paparella D, Notaristefano A, Rubini G. The copper radioisotopes: a systematic review with special interest to ^{64}Cu. *Biomed Res Int* 2014;**786463**.
59. Anderson CJ, Ferdani R. Copper-64 radiopharmaceuticals for PET imaging of cancer: advances in preclinical and clinical research. *Cancer Biother Radiopharm* 2009;**24**(4):379-93.
60. Fischer G, Seibold U, Schirrmacher R, Wangler B, Wangler C. ^{89}Zr, a radiometal nuclide with high potential for molecular imaging with PET: chemistry, applications and remaining challenges. *Molecules* 2013;**18**(6):6469-90.
61. Kam BLR, Teunissen JJM, Krenning EP, de Herder WW, Khan S, van Vliet EI, et al. Lutetium-labelled peptides for therapy of neuroendocrine tumours. *Eur J Nucl Med Mol Imaging* 2012;**39**(1):103-12.
62. Sainz-Esteban A, Prasad V, Schuchardt C, Zachert C, Carril JM, Baum RP. Comparison of sequential planar ^{177}Lu-DOTA-TATE dosimetry scans with ^{68}Ga-DOTA-TATE PET/CT images in patients with metastasized neuroendocrine tumours undergoing peptide receptor radionuclide therapy. *Eur J Nucl Med Mol Imaging* 2012;**39**(3):501-11.

63. Goffredo V, Paradiso A, Ranieri G, Gadaleta CD. Yttrium-90 in the principal radionuclide therapies: an efficacy correlation between peptide receptor radionuclide therapy, radioimmunotherapy and transarterial radioembolization therapy. Ten years of experience (1999-2009). *Crit Rev Oncol Hematol* 2011;**80**(3):393-410.
64. Jeong JM, Chung JK. Therapy with ^{188}Re-labeled radiopharmaceuticals: an overview of promising results from initial clinical trials. *Cancer Biother Radiopharm* 2003;**18**(5):707-17.
65. Hong H, Zhang Y, Sun J, Cai W. Molecular imaging and therapy of cancer with radiolabeled nanoparticles. *Nano Today* 2009;**4**(5):399-413.
66. Barenholz Y. Doxil(R)–the first FDA-approved nano-drug: lessons learned. *J Control Release* 2012;**160**(2):117-34.
67. Seregni EMA, Chiesa C, Scaramellini G, Massimino M, Bombardieri E. Radioiodine therapy of differentiated thyroid cancer. In: Aktolun CGS, editor. *Nuclear medicine therapy*. NY, USA: Springer; 2013. p. 133-53.
68. Parker C, Nilsson S, Heinrich D, Helle SI, O'Sullivan JM, Fosså SD, et al. Alpha emitter radium-223 and survival in metastatic prostate cancer. *N Engl J Med* 2013;**369**(3):213-23.
69. Yong KT, Law WC, Hu R, Ye L, Liu L, Swihart MT, et al. Nanotoxicity assessment of quantum dots: from cellular to primate studies. *Chem Soc Rev* 2013;**42**(3):1236-50.
70. Boisselier E, Astruc D. Gold nanoparticles in nanomedicine: preparations, imaging, diagnostics, therapies and toxicity. *Chem Soc Rev* 2009;**38**(6):1759-82.
71. Xie G, Sun J, Zhong G, Shi L, Zhang D. Biodistribution and toxicity of intravenously administered silica nanoparticles in mice. *Arch Toxicol* 2010;**84**(3):183-90.
72. Khlebtsov N, Dykman L. Biodistribution and toxicity of engineered gold nanoparticles: a review of in vitro and in vivo studies. *Chem Soc Rev* 2011;**40**(3):1647-71.
73. Chen YS, Hung YC, Liau I, Huang GS. Assessment of the in vivo toxicity of gold nanoparticles. *Nanoscale Res Lett* 2009;**4**(8):858-64.
74. de Barros AB, Tsourkas A, Saboury B, Cardoso VN, Alavi A. Emerging role of radiolabeled nanoparticles as an effective diagnostic technique. *EJNMMI Res* 2012;**2**(1):39.
75. Nam J, Won N, Bang J, Jin H, Park J, Jung S, et al. Surface engineering of inorganic nanoparticles for imaging and therapy. *Adv Drug Deliv Rev* 2013;**65**(5):622-48.
76. Baum RP, Prasad V, Müller D, Schuchardt C, Orlova A, Wennborg A, et al. Molecular imaging of HER2-expressing malignant tumors in breast cancer patients using synthetic ^{111}In- or ^{68}Ga-labeled affibody molecules. *J Nucl Med* 2010;**51**(6):892-7.
77. Farokhzad OC, Jon S, Khademhosseini A, Tran T-NT, LaVan DA, Langer R. Nanoparticle-aptamer bioconjugates: a new approach for targeting prostate cancer cells. *Cancer Res* 2004;**64**(21):7668-72.
78. Saw PE, Kim S, I-h Lee, Park J, Yu M, Lee J, et al. Aptide-conjugated liposome targeting tumor-associated fibronectin for glioma therapy. *J Mat Chem B* 2013;**1**(37):4723-6.
79. Ruigrok VJ, Levisson M, Eppink MH, Smidt H, van der Oost J. Alternative affinity tools: more attractive than antibodies? *Biochem J* 2011;**436**(1):1-13.
80. Scott AM, Wolchok JD, Old LJ. Antibody therapy of cancer. *Nat Rev Cancer* 2012;**12**(4):278-87.
81. Kim HK, Kim S, Park JJ, Jeong JM, Mok YJ, Choi YH. Sentinel node identification using technetium-99 m neomannosyl human serum albumin in esophageal cancer. *Ann Thorac Surg* 2011;**91**(5):1517-22.
82. Witzig TE, Gordon LI, Cabanillas F, Czuczman MS, Emmanouilides C, Joyce R, et al. Randomized controlled trial of yttrium-90–labeled ibritumomab tiuxetan radioimmunotherapy versus rituximab immunotherapy for patients with relapsed or refractory low-grade, follicular, or transformed b-cell non-hodgkin's lymphoma. *J Clin Oncol* 2002;**20**(10):2453-63.
83. Wahl RL. Tositumomab and ^{131}I therapy in non-Hodgkin's lymphoma. *J Nucl Med* 2005;**46**(Suppl 1):128S-40S.
84. Hong H, Zhang Y, Severin GW, Yang Y, Engle JW, Niu G, et al. Multimodality imaging of breast cancer experimental lung metastasis with bioluminescence and a monoclonal antibody dual-labeled with ^{89}Zr and IRdye 800cw. *Mol Pharm* 2012;**9**(8):2339-49.
85. Rezaeipoor R, John R, Adie SG, Chaney EJ, Marjanovic M, Oldenburg AL, et al. Fc-directed antibody conjugation of magnetic nanoparticles for enhanced molecular targeting. *J Innov Opt Health Sci* 2009;**2**(4):387-96.
86. Kumar S, Aaron J, Sokolov K. Directional conjugation of antibodies to nanoparticles for synthesis of multiplexed optical contrast agents with both delivery and targeting moieties. *Nat Protoc* 2008;**3**(2):314-20.
87. Cardoso MM, Peca IN, Roque AC. Antibody-conjugated nanoparticles for therapeutic applications. *Curr Med Chem* 2012;**19**(19):3103-27.
88. Wang H, Liu YL, Yang YH, Deng T, Shen GL, Yu RQ. A protein A-based orientation-controlled immobilization strategy for antibodies using nanometer-sized gold particles and plasma-polymerized film. *Anal Biochem* 2004;**324**(2):219-26.
89. Mazzucchelli S, Colombo M, De Palma C, Salvade A, Verderio P, Coghi MD, et al. Single-domain protein a-engineered magnetic nanoparticles: toward a universal strategy to site-specific labeling of antibodies for targeted detection of tumor cells. *ACS Nano* 2010;**4**(10):5693-702.
90. Makaraviciute A, Ramanaviciene A. Site-directed antibody immobilization techniques for immunosensors. *Biosens Bioelectron* 2013;**50**:460-71.
91. Salehi M, Schneider L, Strobel P, Marx A, Packeisen J, Schlucker S. Two-color SERS microscopy for protein co-localization in prostate tissue with primary antibody-protein A/G-gold nanocluster conjugates. *Nanoscale* 2014;**6**(4):2361-7.
92. Dubertret B, Skourides P, Norris DJ, Noireaux V, Brivanlou AH, Libchaber A. In vivo imaging of quantum dots encapsulated in phospholipid micelles. *Science* 2002;**298**(5599):1759-62.
93. Fan H, Yang K, Boye DM, Sigmon T, Malloy KJ, Xu H, et al. Self-assembly of ordered, robust, three-dimensional gold nanocrystal/silica arrays. *Science* 2004;**304**(5670):567-71.
94. Fan H, Leve EW, Scullin C, Gabaldon J, Tallant D, Bunge S, et al. Surfactant-assisted synthesis of water-soluble and biocompatible semiconductor quantum dot micelles. *Nano Lett* 2005;**5**(4):645-8.
95. Wu H, Zhu H, Zhuang J, Yang S, Liu C, Cao YC. Water-soluble nanocrystals through dual-interaction ligands. *Angew Chem Int Ed Engl* 2008;**47**(20):3730-4.
96. Carion O, Mahler B, Pons T, Dubertret B. Synthesis, encapsulation, purification and coupling of single quantum dots in phospholipid micelles for their use in cellular and in vivo imaging. *Nat Protoc* 2007;**2**(10):2383-90.
97. Yang BY, Seelam SR, Young IK, Lee YS, Lee DS, Chung JK, et al. *Preparation of a multimodal iron oxide nanoparticle conjugated with mannose, NOTA and PEG by encapsulation with specific amphiphiles*. Paper presented at: Journal of labelled compounds & radiopharmaceuticals; 2013.
98. Lee DS. *Preparation of multifunctional multimodal nanoparticles using specific amphiphiles: Click chemistry for nanoparticles*. Annual Congress of Clinam (Abstr); 2013.
99. Lee DS. *In vivo application of Cu-64 labeled upconversion nanoparticles*. Annual Congress of Clinam (Abstr); 2014.
100. Samanta A, Maiti KK, Soh KS, Liao X, Vendrell M, Dinish US, et al. Ultrasensitive near-infrared Raman reporters for SERS-based in vivo cancer detection. *Angew Chem Int Ed Engl* 2011;**50**(27):6089-92.
101. Kang H, Jeong S, Park Y, Yim J, Jun BH, Kyeong S, et al. Near-infrared sers nanoprobes with plasmonic Au/Ag hollow-shell assemblies for in vivo multiplex detection. *Adv Funct Mater* 2013;**23**(30):3719-27.
102. Jun BH, Hwang DW, Jung HS, Jang J, Kim H, Kang H, et al. Ultrasensitive, biocompatible, quantum-dot-embedded silica nanoparticles for bioimaging. *Adv Funct Mater* 2012;**22**(9):1843-9.
103. Tomalia DA. In quest of a systematic framework for unifying and defining nanoscience. *J Nanopart Res* 2009;**11**(6):1251-310.

104. Almeida JP, Chen AL, Foster A, Drezek R. In vivo biodistribution of nanoparticles. *Nanomedicine (Lond)* 2011;**6**(5):815-35.
105. Ntziachristos V, Tung CH, Bremer C, Weissleder R. Fluorescence molecular tomography resolves protease activity in vivo. *Nat Med* 2002;**8**(7):757-60.
106. Panagi Z, Beletsi A, Evangelatos G, Livaniou E, Ithakissios DS, Avgoustakis K. Effect of dose on the biodistribution and pharmacokinetics of PLGA and PLGA–mPEG nanoparticles. *Int J Pharm* 2001;**221**(1-2):143-52.
107. Jeong JM, Hong MK, Chang YS, Lee YS, Kim YJ, Cheon GJ, et al. Preparation of a promising angiogenesis PET imaging agent: Ga-68-labeled c(RGDyK)-isothiocyanatobenzyl-1,4,7-triazacyclononane-1,4,7-triacetic acid and feasibility studies in mice. *J Nucl Med* 2008;**49**(5):830-6.
108. Wang Y, Liu Y, Luehmann H, Xia X, Brown P, Jarreau C, et al. Evaluating the pharmacokinetics and in vivo cancer targeting capability of Au nanocages by positron emission tomography imaging. *ACS Nano* 2012;**6**(7):5880-8.
109. Sun X, Huang X, Yan X, Wang Y, Guo J, Jacobson O, et al. Chelator-free cu-integrated gold nanomaterials for positron emission tomography imaging guided photothermal cancer therapy. *ACS Nano* 2014;**8**(8):8438-46.
110. Liu Y, Sun Y, Cao C, Yang Y, Wu Y, Ju D, et al. Long-term biodistribution in vivo and toxicity of radioactive/magnetic hydroxyapatite nanorods. *Biomaterials* 2014;**35**(10):3348-55.
111. Choi HS, Liu W, Misra P, Tanaka E, Zimmer JP, Itty Ipe B, et al. Renal clearance of quantum dots. *Nat Biotechnol* 2007;**25**(10):1165-70.
112. Matsumura Y, Maeda H. A new concept for macromolecular therapeutics in cancer chemotherapy: mechanism of tumoritropic accumulation of proteins and the antitumor agent smancs. *Cancer Res* 1986;**46**(12 Pt 1):6387-92.
113. Maeda H. The enhanced permeability and retention (EPR) effect in tumor vasculature: the key role of tumor-selective macromolecular drug targeting. *Adv Enzyme Regul* 2001;**41**:189-207.
114. Lehner R, Wang X, Marsch S, Hunziker P. Intelligent nanomaterials for medicine: carrier platforms and targeting strategies in the context of clinical application. *Nanomedicine (Lond)* 2013;**9**(6):742-57.
115. Byrne JD, Betancourt T, Brannon-Peppas L. Active targeting schemes for nanoparticle systems in cancer therapeutics. *Adv Drug Deliv Rev* 2008;**60**(15):1615-26.
116. Bartlett DW, Su H, Hildebrandt IJ, Weber WA, Davis ME. Impact of tumor-specific targeting on the biodistribution and efficacy of siRNA nanoparticles measured by multimodality in vivo imaging. *Proc Natl Acad Sci U S A* 2007;**104**(39):15549-54.
117. Arora G, Shukla J, Ghosh S, Maulik SK, Malhotra A, Bandopadhyaya G. PLGA nanoparticles for peptide receptor radionuclide therapy of neuroendocrine tumors: a novel approach towards reduction of renal radiation dose. *PLoS One* 2012;**7**(3):e34019.
118. Karmali PP, Simberg D. Interactions of nanoparticles with plasma proteins: implication on clearance and toxicity of drug delivery systems. *Expert Opin Drug Deliv* 2011;**8**(3):343-57.
119. Cedervall T, Lynch I, Lindman S, Berggård T, Thulin E, Nilsson H, et al. Understanding the nanoparticle–protein corona using methods to quantify exchange rates and affinities of proteins for nanoparticles. *Proc Natl Acad Sci* 2007;**104**(7):2050-5.
120. Monopoli MP, Aberg C, Salvati A, Dawson KA. Biomolecular coronas provide the biological identity of nanosized materials. *Nat Nano* 2012;**7**(12):779-86.
121. Jeong JM, Hong MK, Kim YJ, Lee J, Kang JH, Lee DS, et al. Development of ^{99m}Tc-neomannosyl human serum albumin (^{99m}Tc-MSA) as a novel receptor binding agent for sentinel lymph node imaging. *Nucl Med Commun* 2004;**25**(12):1211-7.
122. Sun M, Sundaresan G, Jose P, Yang L, Hoffman D, Lamichhane N, et al. Highly stable intrinsically radiolabeled indium-111 quantum dots with multidentate zwitterionic surface coating: dual modality tool for biological imaging. *J Mat Chem B* 2014;**2**:4456-66.
123. Semmler-Behnke M, Kreyling WG, Lipka J, Fertsch S, Wenk A, Takenaka S, et al. Biodistribution of 1.4- and 18-nm gold particles in rats. *Small* 2008;**4**(12):2108-11.
124. Lipka J, Semmler-Behnke M, Sperling RA, Wenk A, Takenaka S, Schleh C, et al. Biodistribution of PEG-modified gold nanoparticles following intratracheal instillation and intravenous injection. *Biomaterials* 2010;**31**(25):6574-81.
125. Hirn S, Semmler-Behnke M, Schleh C, Wenk A, Lipka J, Schaffler M, et al. Particle size-dependent and surface charge-dependent biodistribution of gold nanoparticles after intravenous administration. *Eur J Pharm Biopharm* 2011;**77**(3):407-16.
126. Xie H, Wang ZJ, Bao A, Goins B, Phillips WT. In vivo PET imaging and biodistribution of radiolabeled gold nanoshells in rats with tumor xenografts. *Int J Pharm* 2010;**395**(1-2):324-30.
127. Xie J, Chen K, Huang J, Lee S, Wang J, Gao J, et al. PET/NIRF/MRI triple functional iron oxide nanoparticles. *Biomaterials* 2010;**31**(11):3016-22.
128. Xiao Y, Hong H, Javadi A, Engle JW, Xu W, Yang Y, et al. Multifunctional unimolecular micelles for cancer-targeted drug delivery and positron emission tomography imaging. *Biomaterials* 2012;**33**(11):3071-82.
129. Rangger C, Helbok A, Sosabowski J, Kremser C, Koehler G, Prassl R, et al. Tumor targeting and imaging with dual-peptide conjugated multifunctional liposomal nanoparticles. *Int J Nanomedicine* 2013;**8**:4659-71.
130. Souris JS, Lee CH, Cheng SH, Chen CT, Yang CS, Ho JA, et al. Surface charge-mediated rapid hepatobiliary excretion of mesoporous silica nanoparticles. *Biomaterials* 2010;**31**(21):5564-74.
131. Longmire M, Choyke PL, Kobayashi H. Clearance properties of nano-sized particles and molecules as imaging agents: considerations and caveats. *Nanomedicine* 2008;**3**(5):703-17.
132. McNeil SE. Nanoparticle therapeutics: a personal perspective. *Wiley Interdiscip Rev Nanomed Nanobiotechnol* 2009;**1**(3):264-71.
133. Ruggiero A, Villa CH, Bander E, Rey DA, Bergkvist M, Batt CA, et al. Paradoxical glomerular filtration of carbon nanotubes. *Proc Natl Acad Sci U S A* 2010;**107**(27):12369-74.
134. Yu T, Hubbard D, Ray A, Ghandehari H. In vivo biodistribution and pharmacokinetics of silica nanoparticles as a function of geometry, porosity and surface characteristics. *J Control Release* 2012;**163**(1):46-54.
135. Cho WS, Cho M, Jeong J, Choi M, Cho HY, Han BS, et al. Acute toxicity and pharmacokinetics of 13 nm-sized PEG-coated gold nanoparticles. *Toxicol Appl Pharmacol* 2009;**236**(1):16-24.
136. Cho WS, Cho M, Jeong J, Choi M, Han BS, Shin HS, et al. Size-dependent tissue kinetics of PEG-coated gold nanoparticles. *Toxicol Appl Pharmacol* 2010;**245**(1):116-23.
137. Terentyuk GS, Maslyakova GN, Suleymanova LV, Khlebtsov BN, Kogan BY, Akchurin GG, et al. Circulation and distribution of gold nanoparticles and induced alterations of tissue morphology at intravenous particle delivery. *J Biophotonics* 2009;**2**(5):292-302.
138. Balasubramanian SK, Jittiwat J, Manikandan J, Ong CN, Yu LE, Ong WY. Biodistribution of gold nanoparticles and gene expression changes in the liver and spleen after intravenous administration in rats. *Biomaterials* 2010;**31**(8):2034-42.
139. Gao H, Xiong J, Cheng T, Liu J, Chu L, Ma R, et al. In vivo biodistribution of mixed shell micelles with tunable hydrophilic/hydrophobic surface. *Biomacromolecules* 2013;**14**(2):460-7.
140. Szebeni J, Bedocs P, Rozsnyay Z, Weiszhar Z, Urbanics R, Rosivall L, et al. Liposome-induced complement activation and related cardiopulmonary distress in pigs: factors promoting reactogenicity of Doxil and Am Bisome. *Nanomedicine (Lond)* 2012;**8**(2):176-84.
141. Beutler BA. TLRs and innate immunity. *Blood* 2009;**113**(7):1399-407.
142. Seong S-Y, Matzinger P. Hydrophobicity: an ancient damage-associated molecular pattern that initiates innate immune responses. *Nat Rev Immunol* 2004;**4**(6):469-78.
143. Matzinger P, Kamala T. Tissue-based class control: the other side of tolerance. *Nat Rev Immunol* 2011;**11**(3):221-30.

144. O'Neill LA, Golenbock D, Bowie AG. The history of Toll-like receptors – redefining innate immunity. *Nat Rev Immunol* 2013;**13**(6):453-60.
145. Turabekova M, Rasulev B, Theodore M, Jackman J, Leszczynska D, Leszczynski J. Immunotoxicity of nanoparticles: a computational study suggests that CNTs and C60 fullerenes might be recognized as pathogens by Toll-like receptors. *Nanoscale* 2014;**6**(7):3488-95.
146. Ho CC, Luo YH, Chuang TH, Yang CS, Ling YC, Lin P. Quantum dots induced monocyte chemotactic protein-1 expression via MyD88-dependent Toll-like receptor signaling pathways in macrophages. *Toxicology* 2013;**308**:1-9.
147. Cejudo-Guillen M, Ramiro-Gutierrez ML, Labrador-Garrido A, Diaz-Cuenca A, Pozo D. Nanoporous silica microparticle interaction with toll-like receptor agonists in macrophages. *Acta Biomater* 2012;**8**(12):4295-303.
148. Chen GY, Yang HJ, Lu CH, Chao YC, Hwang SM, Chen CL, et al. Simultaneous induction of autophagy and toll-like receptor signaling pathways by graphene oxide. *Biomaterials* 2012;**33**(27):6559-69.
149. Yazdi AS, Guarda G, Riteau N, Drexler SK, Tardivel A, Couillin I, et al. Nanoparticles activate the NLR pyrin domain containing 3 (Nlrp3) inflammasome and cause pulmonary inflammation through release of IL-1α and IL-1β. *Proc Natl Acad Sci* 2010;**107**(45):19449-54.
150. Sun B, Wang X, Ji Z, Li R, Xia T. NLRP3 inflammasome activation induced by engineered nanomaterials. *Small* 2013;**9**(9-10):1595-607.
151. Moyano DF, Goldsmith M, Solfiell DJ, Landesman-Milo D, Miranda OR, Peer D, et al. Nanoparticle hydrophobicity dictates immune response. *J Am Chem Soc* 2012;**134**(9):3965-7.
152. Thompson Elizabeth A, S BC, Glista-Baker Ellen E, Shipkowski Kelly A, Taylor Alexia J, Bonner James C. Innate immune responses to nanoparticle exposure in the lung. *J Environ Immunol Toxicol* 2014;**2**(1):46-52.
153. Mizrahy S, Raz SR, Hasgaard M, Liu H, Soffer-Tsur N, Cohen K, et al. Hyaluronan-coated nanoparticles: the influence of the molecular weight on CD44-hyaluronan interactions and on the immune response. *J Control Release* 2011;**156**(2):231-8.
154. Mora-Solano C, Collier JH. Engaging adaptive immunity with biomaterials. *J Mater Chem B Mater Biol Med* 2014;**2**(17):2409-21.
155. Smith MJ, Brown JM, Zamboni WC, Walker NJ. From immunotoxicity to nanotherapy: the effects of nanomaterials on the immune system. *Toxicol Sci* 2014;**138**(2):249-55.
156. Schellekens H, Hennink WE, Brinks V. The immunogenicity of polyethylene glycol: facts and fiction. *Pharm Res* 2013;**30**(7):1729-34.
157. Ishida T, Wang X, Shimizu T, Nawata K, Kiwada H. PEGylated liposomes elicit an anti-PEG IgM response in a T cell-independent manner. *J Control Release* 2007;**122**(3):349-55.
158. Rodriguez PL, Harada T, Christian DA, Pantano DA, Tsai RK, Discher DE. Minimal "Self" peptides that inhibit phagocytic clearance and enhance delivery of nanoparticles. *Science* 2013;**339**(6122):971-5.
159. Oltra NS, Nair P, Discher DE. From stealthy polymersomes and filomicelles to "self" peptide-nanoparticles for cancer therapy. *Annu Rev Chem Biomol Eng* 2014;**5**:281-99.
160. Adiseshaiah PP, Hall JB, McNeil SE. Nanomaterial standards for efficacy and toxicity assessment. *Wiley Interdiscip Rev Nanomed Nanobiotechnol* 2010;**2**(1):99-112.
161. Johnston HJ, Semmler-Behnke M, Brown DM, Kreyling W, Tran L, Stone V. Evaluating the uptake and intracellular fate of polystyrene nanoparticles by primary and hepatocyte cell lines in vitro. *Toxicol Appl Pharmacol* 2010;**242**(1):66-78.
162. Bergen JM, von Recum HA, Goodman TT, Massey AP, Pun SH. Gold nanoparticles as a versatile platform for optimizing physicochemical parameters for targeted drug delivery. *Macromol Biosci* 2006;**6**(7):506-16.
163. Chen H, Wang L, Yeh J, Wu X, Cao Z, Wang YA, et al. Reducing non-specific binding and uptake of nanoparticles and improving cell targeting with an antifouling PEO-b-PgammaMPS copolymer coating. *Biomaterials* 2010;**31**(20):5397-407.
164. Pavot V, Rochereau N, Primard C, Genin C, Perouzel E, Lioux T, et al. Encapsulation of Nod1 and Nod2 receptor ligands into poly(lactic acid) nanoparticles potentiates their immune properties. *J Control Release* 2013;**167**(1):60-7.
165. Jenkins JT, Halaney DL, Sokolov KV, Ma LL, Shipley HJ, Mahajan S, et al. Excretion and toxicity of gold-iron nanoparticles. *Nanomedicine* 2013;**9**(3):356-65.
166. Johnston HJ, Hutchison G, Christensen FM, Peters S, Hankin S, Stone V. A review of the in vivo and in vitro toxicity of silver and gold particulates: particle attributes and biological mechanisms responsible for the observed toxicity. *Crit Rev Toxicol* 2010;**40**(4):328-46.
167. Ishida T, Harashima H, Kiwada H. Liposome clearance. *Biosci Rep* 2002;**22**(2):197-224.
168. Ishida T, Ichihara M, Wang X, Kiwada H. Spleen plays an important role in the induction of accelerated blood clearance of PEGylated liposomes. *J Control Release* 2006;**115**(3):243-50.
169. Beer AJ, Haubner R, Wolf I, Goebel M, Luderschmidt S, Niemeyer M, et al. PET-based human dosimetry of ^{18}F-galacto-RGD, a new radiotracer for imaging alpha v beta3 expression. *J Nucl Med* 2006;**47**(5):763-9.
170. Liu N, Li M, Li X, Meng X, Yang G, Zhao S, et al. PET-based biodistribution and radiation dosimetry of epidermal growth factor receptor-selective tracer 11C-PD153035 in humans. *J Nucl Med* 2009;**50**(2):303-8.